UNIVERSITY OF EDUCATION, WINNEBA

COLLEGE OF TECHNOLOGY EDUCATION, KUMASI

AN EXPERIMENTAL STUDY INTO THE EFFECTS OF BENDING ON THE

MECHANICAL PROPERTIES OF MILD (AISI 1018) STEEL PIPES

YUSSIF BASHIRU

OCTOBER, 2020

UNIVERSITY OF EDUCATION, WINNEBA

COLLEGE OF TECHNOLOGY EDUCATION, KUMASI

AN EXPERIMENTAL STUDY INTO THE EFFECTS OF LOAD ON THE MECHANICAL PROPERTIES OF MILD STEEL PIPES (AISI 1018) PIPES

YUSSIF BASHIRU

(200029715)

A Thesis in the Department of MECHANICAL AND AUTOMOTIVE TECHNOLOGY EDUCATION, Faculty of Technical Education, Submitted to the School of Graduate Studies, University of Education Winneba, in partial fulfillment of the requirements for the award of Master of Philosophy (Mechanical Engineering Technology) degree

OCTOBER, 2020

DECLARATION

Student's Declaration

I, YUSSIF BASHIRU, declare that this Thesis, with the exception of the quotations and references contained in the published works which have all been identified and duly acknowledged, is entirely my own original, and it has not been submitted either in part or whole for another degree elsewhere.

SIGNATURE:…………………………………

DATE:………………………………………………

SUPERVISOR'S DECLARATION

I hereby declare that the preparation and presentation of this work was supervised in accordance with the guidelines for supervision of Thesis as laid down by the University of Education, Winneba.

NAME OF SUPERVISOR: Dr. KWABENA OFFEH GYIMAH

SIGNATURE:…………………………………..

DATE:…………………………………………..

ACKNOWLEDGEMENT

I thank God Almighty for His protection throughout this study. His Grace has been abundant. My sincerest gratitude goes to my supervisor, Dr. Kwabena Offeh Gyimah for his immense guidance. Sir, may the good Lord richly bless you for your wonderful supervision. My profound appreciation goes to the Department of Mechanical and Automotive Technology Workshop at Akenten Appiah-Minkah University of Skills Training and Entrepreneurial Development (AAMUSTED), Kumasi and the CBT Construction laboratory for the assistance offered me during the study. I am very grateful to everyone who played diverse roles to make this study a success.

May the good Lord bless you.

DEDICATION

This work is dedicated to the Glory of God.

TABLE OF CONTENTS

Content	Page

LIST OF TABLES

Content   **Page**

LIST OF FIGURES

Content   **Page**

ABSTRACT

AISI 1018 mild steel is a versatile industrial material due to its excellent mechanical properties and numerous industrial applications. It possesses a good balance of high strength, ductility, weldability, and excellent thermal and electrical conductivity. Just like other industrial materials, mechanical components made from mild steel are susceptible to fracture or cracks when subjected to varying loading or stress conditions. This study therefore used experimental method to investigate the effect of bending on the mechanical properties of mild steel (AISI 1018). The test samples were prepared based on the standards of American Iron and Steel Institute (AISI). The findings of the study showed that, with the exception of the percentage strain (which increased averagely for L, C and S samples by 0.122%, 0.2895% and 0.06% respectively), the bending and welding samples adversely affected the other mechanical properties studied; (i.e. Ultimate Tensile Strength, Yield Strength, Elastic Moduli, impact and deformation characteristics) of the samples witnessed reductions in values after bending, welding and testing. This increase in strain of the welded sample L- shape is attributable to the heat induced during the electric arc welding processes and the bending of the C – shape samples. The study also showed that, the grain size of the samples improved in the welded sample L; as there was a near even distribution of dark and gray spots in the micrographs. The findings of this study could therefore help metal fabrication professionals and regulators to appreciate the impact of bending and electric arc welding on the microstructure and mechanical properties of mild steel pipe components and structures. Also, it may assist industry regulators to promulgate standards to regulate the bending and welding of mild steel and possibly other industrial materials in order to preserve the natural properties of the materials.

CHAPTER ONE

INTRODUCTION

1.1 Background to the Study

The most common effects of bending on the mechanical properties of circular and square pipes are deformation and fracture. Most industries use bent pipes as air conditioning, boiler, power generation, ship building, furniture, railroad, automotive, off-road, farm equipment and aircraft. Steel is one of the vital materials used in the construction of roads, railways, other infrastructure, appliances, and buildings. Steel is used in a variety of other construction materials, such as bolts, nails, and screws. Pipe bends are frequently used to change the direction in pipeline systems and they are considered one of the critical components as well. Bending moments acting on the pipe bends result from the surrounding environment, such as thermal expansions, deformations, and external loads. As a result of these bending moments, the initially circular cross-section of the pipe bend deforms into an oval shape. This consequently changes the pipe bend's flexibility leading to higher stresses compared to straight pipes (Abdul hameed, Martens, Cheng & Adeeb, 2017). Pipe bends and elbows are one of the most important components used to change the direction in a pipeline. The pipe bend is often one of the most critical components in any pipeline system and it is the location where the high stresses are usually found (Abdul hameed, Martens, Cheng & Adeeb, 2017). The main reason for the high stress levels in a bend is due to its high flexibility since the initially circular cross-section has the ability to deform when subjected to bending, which tends to increase the flexibility and leads to an increase in the stress levels. This is known as the ―Ovalization effect". The ovalization effect was covered in past studies for bends under closing in-plane bending moment (Clark & Reissner. 1951; Rodabaugh. George, & Louisville,1957).

1

Karman, (1911) was the first to relate the flexibility of the bend to its cross-sectional deformation and introduced the idea of a flexibility factor (K). It was found that a straight pipe is stiffer than a pipe bend since it will not undergo any cross-sectional deformation (Ovalization) when subjected to bending. Following this initial study by Karman (1911), many studies were conducted to develop a factor to account for the high stress levels. Clark and Reissner, (1951), conducted extensive studies for 90-degree bends subjected to closing in-plane bending moment and proposed flexibility factors (K) and stress intensification factors (i) that are currently used by the codes [ASME B31.Von Karman, Th. (1911). ASME B31.3 and CSA Z662-15. Although, these factors were derived for a 90-degree pipe bend subjected to in-plane closing bending moment, yet they are still used without modification for other loading cases such as in- plane opening moment or out-of-plane moment L.

In Asnawi, et al. (2004)'s paper, an approach to understand the effect of the in-plane bending moment direction and its influence on the stress levels is conducted. A numerical model is conducted for pipe elbows with different nominal pipe size (NPS), bend radius (R) and bend angles (α) subjected to opening or closing in-plane bending moment. The study shows that the direction of bending has a significant effect on the stress distribution on the pipe elbow. In addition, the stiffness of the pipe bend is affected as well by the bending moment direction.

In this project, the effect of load impact on bend pipes was studied; and the mild steel was prepared as a work piece. The tensile test experiment on bend pipes was conducted in order to determine the effect of load impact on the mild steels work piece. After the Tensile Test experiment, the stress Strain graph was used as a guide to analyse the yield strength, ultimate tensile stress, Fracture Stress and young Modulus.

The subject of mechanical testing of materials is an important aspect of engineering practice. Today, more concern is being given to the interpretation of test results in terms of service performance, as well as giving reliable indications of the ability of the material to perform certain types of duty. Mechanical tests are also employed in investigational work in order to obtain data for use in design to ascertain whether the material meets the specifications for its intended use (Rao, 2011).

1.2 Statement of the Problem

Due to the high carbon content present in mild steel materials, components and parts made from mild steel are ductile and brittle. Hence mechanical components made from square and circular bent pipes may develop cracks, fracture and sometimes even break as a result of fatigue, impact loading and stress concentrations at critically loaded bent pipes and welded components. A study shows that the direction of bending has a significant effect on the stress distribution on the pipe elbow, and the stiffness of the pipe bend is affected as well by the bending moment direction (Asnawi, et al., 2004).

This may necessitate for such defective components to be repaired and one of the widely used methods of correcting such defects is evenly heating and cooling the bent pipe locally during welding, designing the bent pipe fittings with a large bending radius as much as possible.

During electric-arc welding processes, thermal stresses and possible defects in the weld may tend to affect the microstructure, strength and the mechanical properties of the parent materials (High Carbon Steel) which could subsequently affect the integrity and elemental make-up of the base or parent metal.

Again, mechanical components made from square and circular bent pipes usually develop dents, cracks and fracture and sometimes even split which leads to failure. The failure is irrespective of whether the bent is a welded joint or non-welded joint. What then is the cause of this failure? Is it as a result of fatigue, impact loading or stress concentrations or what? There is the need for an empirical study to be conducted to find answers to these questions.

Hence, an experimental study needs to be conducted to ascertain the effect of load on the mechanical properties of both the bended and the welded mild steel pipes (AISI 1018).

1.3 Purpose of the study

This study therefore sought to experimentally investigate the extent to which the mechanical properties of mild steel pipes (yield strength, ultimate tensile stress, fracture stress, young modulus) as well as the deformation and fracture characteristics are affected after being subjected to tensile loads.

The following specific research objectives were formulated to guide the study;

1. To determine the load-displacement/stress-strain relationship of welded mild steel pipes,

2. To examine the load-displacement/stress-strain relationship of bent mild steel pipe

3. To evaluate the mechanical properties of Bent and welded mild steel pipes

4. To compare the deformation and fracture characteristics of bent and welded mild steel pipes

1.4 Significance of the study

The findings of this study may help the metal fabrication industry professionals and regulators to appreciate the changes that occur in square mild steel pipes after being bent or welded, and how such effects could be minimized, if not eliminated entirely. The findings of this study may also assist industry regulators to enact legislations to regulate the extent to which loads are exerted on Bent and welded mild steel pipes used in welding structural and machine components.

1.5 Limitations of the Study

Due to time constraints the study used only the square mild steel pipes though it would have been appropriate to compare the mechanical properties of both square and circular mild steel pipes. There were only two centres available for the experimental testing of the hardness of the samples used. However due to the breakdown of the machines in those centres, the experiment could not be carried out. As a result, the Solidworks Simulation software was used to determine the impact analysis of the bent and welded samples.

1.6 Outline of the study

Chapter 1 introduces the background, problem statement and the scopes of this study. Chapter 2 presents the literature study about material used, mechanical properties and deformation and fracture characteristics of mild steel pipes. Chapter 3 discusses the materials and methods used for the study. Chapter 4 discusses the results and analysis of the tensile test experiment and impact test. Chapter 5 presents the summary of findings, conclusion, recommendation and suggestion for future work.

CHAPTER TWO

LITERATURE REVIEW

2.1 Introduction

This literature review covers the following relevant areas: Mild steel, Uniaxial tensile testing, Stress and strain relationship, Mechanical properties of mild steel pipes under Tensile Testing, Deformation and fracture characteristics of mild steel pipes.

2.2 Mild steel

Mild steel is a type of steel alloy that contains a high amount of carbon as a major element. An alloy is a mixture of metals and non-metals, designed to have specific properties (Zarif et.al., 2012). Alloys make it possible to compensate for the shortcomings of a pure metal by adding other elements. To get what mild steel is, one must know what alloys that are combined to make steel. Steel is any alloy of iron, consisting of 0.2% to 2.1% of carbon, as a hardening agent. Besides carbon, there are many metal elements that are part of steel alloys. The elements other than iron and carbon, used in steel are chromium, manganese, tungsten and vanadium. All these elements along with carbon, act as hardening agents. That is, they prevent dislocations from occurring inside the iron crystals and prevent the lattice layers from sliding past each other. This is what makes steel harder than iron. Varying the amounts of these hardening agents creates different grades of steel. The ductility, hardness and mild steel tensile strength are a function of the amount of carbon and other hardening agents, present in the alloy. The amount of carbon is a deciding factor, which decides hardness of the steel alloy. A steel alloy with a high carbon content is mild steel, which is in fact, much harder and stronger than iron. Though, increased carbon content increases the hardness of the steel alloy (Zarif et. Al., 2012).

6

2.2.1 Types of Mild Steel

(a) 1018 Mild Steel

Alloy 1018 is the most commonly available of the cold-rolled steels. It is generally available in round rod, square bar, and rectangle bar. It has a good combination of all of the typical traits of steel strength, some ductility, and comparative ease of machining. Chemically, it is very similar to A36 Hot Rolled steel, but the cold rolling process creates a better surface finish and better properties (Zarif & Malek, 2012).

Table 2.1: Mechanical Properties of 1018 Mild (low-carbon) Steel

Minimum Properties	Ultimate tensile Strength, psi	63,800
	Yield strength, psi	53,700
	Elongation	15.0%
	Rockwell Hardness	B71
Chemistry	Iron (Fe)	98.81 – 99.26%
	Carbon (C)	0.18%
	Manganese (Mn)	0.6 – 0.9%
	Phosphorus (P)	0.04% max
	Sulphur (S)	0.05% max

Source: (Zarif & Malek, 2012).

Few studies related to the mechanical properties of mild steel AISI 1018 manufactured via the cold-drawing process at elevated temperatures indicated that, high-strength CDS AISI 1018 in a round bar shape with highly deformed lamellar pearlite microstructures containing ferrite can be used in reinforced concrete structures, especially with a diameter of 5–12mm as the main load-bearing bars of the slab members (Zong, 2015 and Shakya, 2016). In addition, cold-drawn steel tubes can be used as an alternative to welded and cold-rolled steel tubes because cold-drawn steel products exhibit narrower ranges of tolerance and section properties, which

7

enables less machining and improved straightness. It is well known that at elevated temperatures, structural steel grades with ferrite–pearlite microstructures undergo lower reduction in steel strength than HSS and VHS steel grades with martensite microstructures (Heidarpour et al. 2014). Therefore, the study of the mechanical behaviour of CDS AISI 1018 at elevated temperatures regarding structural fire-engineering design applications is of considerable importance for providing data regarding cold-drawn AISI 1018 steel under steady-state high-temperature conditions.

(b) A36 Mild Steel

ASTM A36 steel is the most commonly available of the hot-rolled steels. It is generally available in round rod, square bar, rectangle bar, as well as steel shapes such as I - Beams, H-beams, angles, and channels. The hot roll process means that the surface on this steel will be somewhat rough. Note that its yield strength is also significantly less than 1018. This means that it will bend much more quickly than will 1018. Finally, machining this material is noticeably more difficult than 1018 steel, but the cost is usually significantly lower (Zarif & Malek, 2012).

Table 2.2: Mechanical Properties of A36 Mild Steel

Minimum Properties	Ultimate tensile Strength, psi	58,000 – 79,800
	Yield strength, psi	36,300
	Elongation	20.0%
Chemistry	Iron (Fe)	99%
	Carbon (C)	0.26%
	Manganese (Mn)	0.75%
	Copper (Cu)	0.2%
	Phosphorus (P)	0.04% max
	Sulphur (S)	0.05% max

Source: (Zarif & Malek, 2012).

2.3 Uniaxial tensile testing

Uniaxial tensile test is known as a basic and universal engineering test to achieve material parameters such as ultimate strength, yield strength, % elongation, % area of reduction and Young's modulus. These important parameters obtained from the standard tensile testing are useful for the selection of engineering materials for any applications required (Hashemi, 2006). Also, according to Callister (2007), tensile testing is a designed laboratory experiments that duplicate service conditions, and the experimental results and present the mechanical behavior on a graph. Test results are displayed as nominal stress versus nominal strain, as "the mechanical behavior of a material reflects the relationship between its response or deformation to an applied load or force" (Callister, 2007). Tensile testing slowly applies incremental axial (quasi-static) load to specimen materials that primarily respond in uniaxial tension. The experimental process is continued with increased uniaxial load until reaching a desired level of deformation or the test specimen is fractured.

In addition, a standard specimen is prepared in a round or a square section along the gauge length as shown in figures 2.1 (a) and 2.1(b) respectively, depending on the standard used. Both ends of the specimens should have sufficient length and a surface condition such that they are firmly gripped during testing.
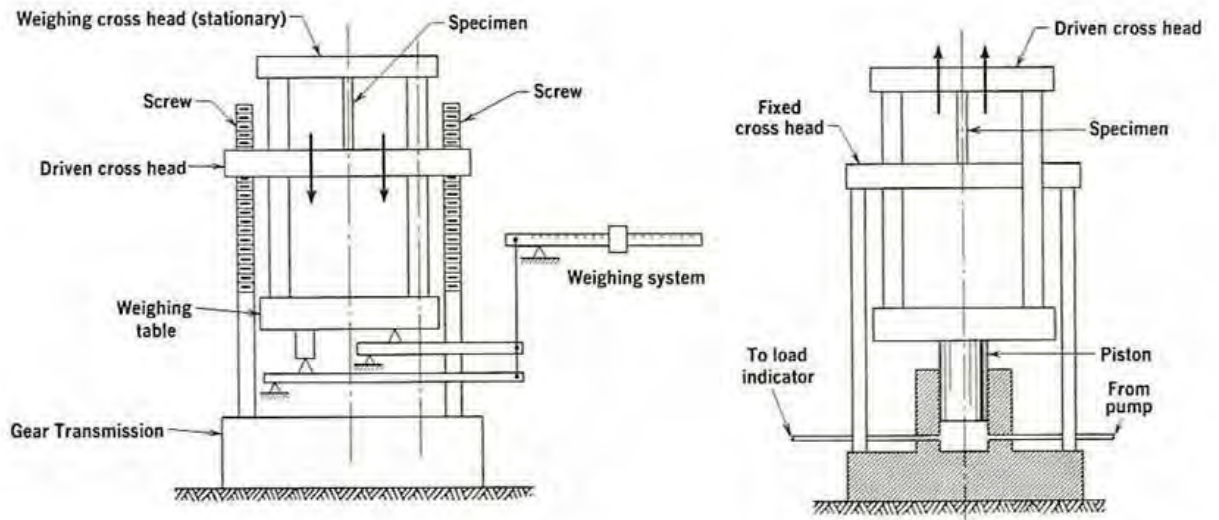
Figure 2.1: Schematics (a) a screw driven machine (b) a hydraulic testing machine (Callister, 2001)

The equipment used for tensile testing ranges from simple devices to complicated controlled systems. The so-called universal testing machines are commonly used, which are driven by mechanical screw or hydraulic systems. Figure 2.1a, illustrates a relatively simple screw-driven machine using large two screws to apply the load whereas figure 2.1b, shows a hydraulic testing machine using the pressure of oil in a piston for load supply. These types of machines can be used not only for tension, but also for compression, bending and torsion tests. A more modernized closed-loop servo-hydraulic machine provides variations of load, strain, or testing machine motion (stroke) using a combination of actuator rod and piston. Most of the machines used nowadays are linked to a computer-controlled system in which the load and extension data can be graphically displayed together with the calculations of stress and strain.

General techniques utilized for measuring loads and displacements employs sensors providing electrical signals. Load cells are used for measuring the load applied while strain gauges are used for strain measurement. A Change in a linear dimension is

proportional to the change in electrical voltage of the strain gauge attached on to the specimen. The initial gauge length Lo is standardized (in several countries) and varies with the diameter (Do) or the cross-sectional area (Ao) of the specimen as listed in table 2.3. This is because if the gauge length is too long, the % elongation might be underestimated in this case. Any heat treatments should be applied on to the specimen prior to machining to produce the final specimen readily for testing. This has been done to prevent surface oxide scales that might act as stress concentration which might subsequently affect the final tensile properties due to premature failure.

Table 2.3: Dimensional relationships of tensile specimens used in different countries

TYPE SPECIMEN	UNITED STATE(ASTM)	GREAT BRITAIN	GERMAN
Sheet ($L_0 / \sqrt{A_0}$)	4.5	5.65	11.3
Rod ($L_0 / \sqrt{D_0}$)	4.0	5.0	10.0

Source: (ASTM E8/E8M, 2015).

According to ASTM E8/E8M (2015), material use and selection is important to ensure material properties are strong and rigid enough to withstand actual loads under a variety of conditions. Material characteristics may be sensitive to size and shape of specimen, time, temperature, and condition of the testing machine. In order to avoid factors that will influence the testing result, experiments follow common standards and procedures which have been published by the American Standard of Testing Materials (ASTM) International. For instance, ASTM E8: is a standard test method for tension testing of metallic materials and ASTM B557 is standard test methods of tension testing wrought and cast aluminium and magnesium alloy products (ASTM E8/E8M, 2015).

The strength of material depends on its ability to sustain a load without undue deformation or failure. This property is inherent in the material itself and must determine by experiment. One of the most important tests to perform in this regard is the tension or compression test. Although many important mechanical properties can be determined from this test, it is used to determine the relationship between the average normal stress and average normal strain in many engineering materials such as metals, ceramics, polymers and composites (Chen, 2016).

Tensile test is used to evaluate the strength of metals and alloys. In this test a metal & plastic sample is pulled to failure in a relatively short time at a constant rate. Before testing, two small punch marks are identified along the specimen's length. The ability of a material to resist breaking under tensile stress is one of the most important and widely measured properties of materials used in structural applications (Chen, 2016).

The mechanical properties of a material are related to its behaviour when subjected to continuously increasing elongations up to rupture or fracture. A thorough understanding of a material's mechanical properties is required for engineers if catastrophic failures are to be avoided. The Tensile Test is a common standard test and is a valuable method of determining important mechanical properties of engineering materials (Gedney, 2002).

2.4 Stress and Strain relationship

Stress-strain curve is the output of tensile testing and it describes two important concepts: mechanics of materials and mechanics of deformable bodies. The stress-strain is usually plotted as load/force corresponding to elongation, with the stress along the y-axis and the strain along the x-axis. ―It is desirable to plot the data, results

12

of tensile testing, of the stress-strain curve if the results are to be used to predict how a metal will behave under other forms of loading" (Chen, 2016).

The basic curve can be divided into two regions: elastic and plastic. In basic engineering design, the material starts in linear elastic region. In the elastic region, the tensile stress is proportional to the strain with the constant of proportionality, and the stress-strain curve is linear. This linear relationship was found by Sir Robert Hooke in 1678, which is also called Hook's law, and most materials comply to Hook's law with reasonable approximation in the early portion of the stress-strain curve (Beer et al., 2015). In addition, the material's deformation involves several stages before breakage, including un-deformed state, elastic point, yield point, strain hardening, maximum stress point, and failure as shown in Figure 2.2. During the tensile test, the applied load is measured by a load cell, and the resulting material ductility is recorded by attached extensometer or strain gage.
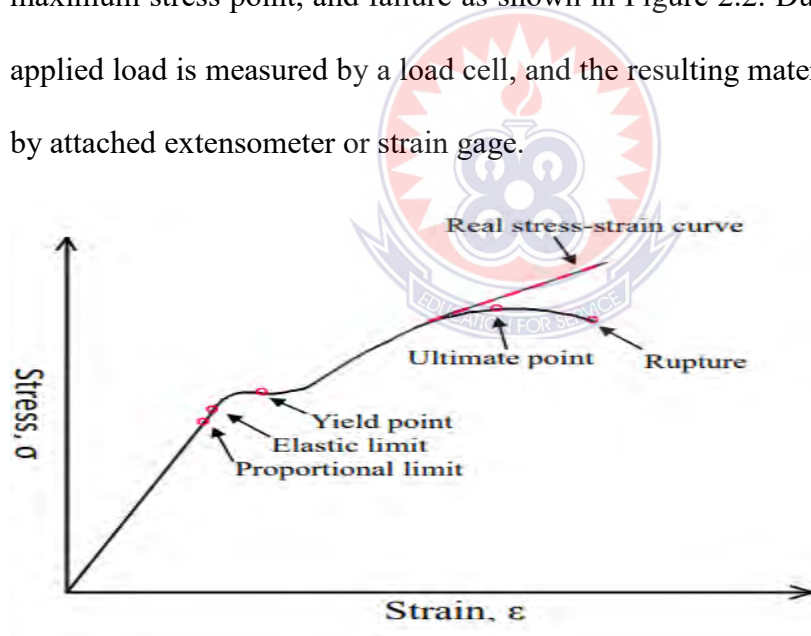
Figure 2.2: Stress-strain relationship under uniaxial tensile loading

2.5 Mechanical Properties of Mild Steel

2.5.1 Yield strength (stress)

By considering the stress-strain curve beyond the elastic portion, if the tensile loading continues, yielding occurs at the beginning of plastic deformation. The yield stress,

σy, can be obtained by dividing the load at yielding (Py) by the original cross-sectional area of the specimen (Ao) as shown in Eq. (2.1).

$$\sigma = \frac{P_y}{A_o} \qquad\qquad (2.1)$$

The yield strength, which indicates the onset of plastic deformation, is considered to be vital for engineering structural or component designs where safety factors are normally used as shown in eq. (2.2)

$$\sigma_w = \frac{\sigma_y}{FoS} = \frac{\sigma_{TS}}{FoS} \qquad\qquad (2.2)$$

For instance, if the allowable working strength σ w = 500 MPa to be employed with a safety factor of 1.8, the material with a yield strength of 900 MPa should be selected. It should be noted that the yield strength value can also be replaced by the ultimate tensile strength, σ TS, for engineering design (Callister, 2001). Safety factors are based on several considerations; the accuracy of the applied loads used in the structure or components, estimation of deterioration, and the consequences of failed structures (loss of life, financial, economic loss, etc.) (Callister, 2001). Generally, buildings require a safety factor of 2, which is rather low since the load calculation has been well understood. Automobiles has safety factor of 2 while pressure vessels utilize safety factors of 3.

It is hard to define the yield point, because some materials lack the existence of a sharp knee or discontinuity. Hence the deviation from the proportionality of stress to strain could be indicated by the offset method, or stress at around 1% strain. The offset method is accomplished by constructing the straight line of slope E (line AC in Figure 2.3) and drawing the line BD parallel to line AC, spaced by the proper amount of permanent strain (AB) — 0.2% being commonly applied for most metallic materials (ASTM A370, 2014). Then, yield strength, σy, is located by finding point E,

which is on the intersection of the line BD and stress-strain curve as it bends through the inelastic range. This construction is shown in Figure 2.3, with point F representing the value of yield strength.
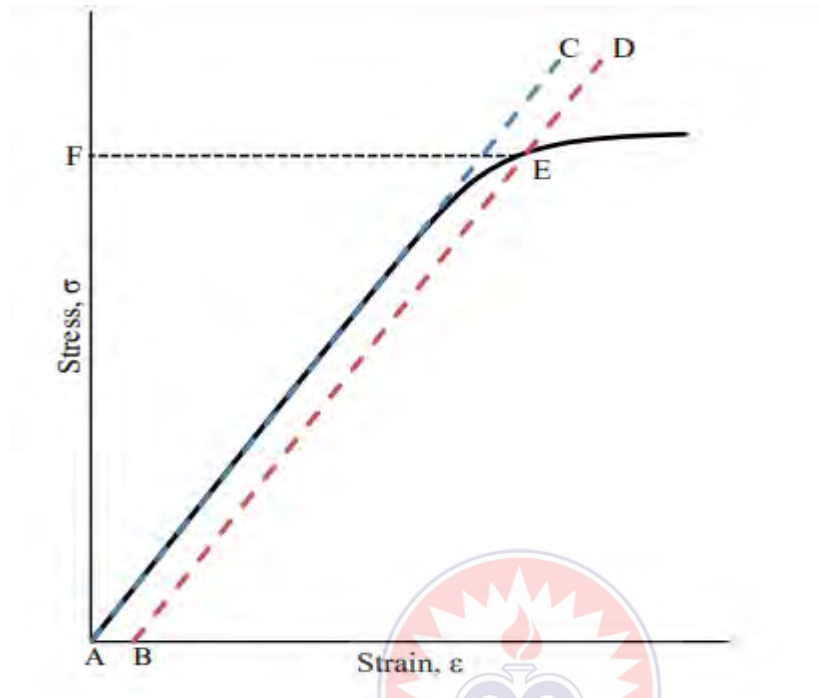
Figure 2.3: Offset methods for determination of yield strength on σ-ε curve.

Additionally, in ASTM A881 ― the ―standard specification for steel wire, indented, low relaxation for prestressed concrete railroad ties", specifically identifies yield strength for this type of prestressing wire to fall at the load corresponding to 1% extension (ASTM A881/A881M, 2015).

2.5.2 Yield Point

As stated in the ASTM A370 standard, ―Yield point is the first stress in a material, less than the maximum obtainable stress, at which an increase in strain occurs without an increase in stress" (ASTM A370, 2014). Beyond the yield point, or plastic region, the material deformation is plastic or permanent, and the stress is no longer proportional to the strain (Callister, 2007). The yield point is an important tensile

15

property, since it is desirable to know whether or not the structure has the capability to function where and when yielding occurs. ―If the stress-strain diagram is characterized by a sharp knee or discontinuity," the yield point can be determined by one of the following methods according to ASTM A370 (2014): Drop-of-the-beam or halt-of-pointer method , Autographic-diagram method and Total extension-under-load method (EUL).

When the tested material does not exhibit a clear yield point, the EUL method with a recorded machine may be the proper approach. When applying this approach, the yield point is not more than 80 ksi (551.58 MPa) and total extension is limited to approximately 0.005 in (0.127 mm) (ASTM A370, 2014). For the exception that if the force is beyond 80 ksi (551.58 MPa), the limiting total extension should be increased as mentioned in ASTM A370 (2014).

2.5.3 Ultimate tensile stress

Beyond yielding, continuous loading leads to an increase in the stress required to permanently deform the specimen as shown in the engineering stress-strain curve in figure 2.3. At this stage, the specimen is strain hardened or work hardened. The degree of strain hardening depends on the nature of the deformed materials, crystal structure and chemical composition, which affects the dislocation motion. FCC structure materials having a high number of operating slip systems can easily slip and create a high density of dislocations. Tangling of these dislocations requires higher stress to uniformly and plastically deform the specimen, therefore resulting in strain hardening.

If the load is continuously applied, the stress-strain curve will reach the maximum point, which is the ultimate tensile strength (UTS σTS). At this point, the specimen can withstand the highest stress before necking takes place.

$$\sigma_{TS} = \frac{P_{\max}}{A_o} \qquad\qquad (2.3)$$

The stress-strain curve continues to develop after yielding and plastic deformation of the material, until reaching maximum stress before decreasing to eventual fracture. Ultimate strength, σu, is the highest point on the stress-strain curve and is the strength the structure can sustain in tension (Whitney, 1937 as cited in Yuszu 2016). After the material reaches the uppermost point on the stress-strain curve, necking phenomenon initiates. Necking occurs shortly before final rupture. The material's cross-sectional area reduces, and the specimen becomes weakened during the necking process (Byars, et. al., 1925 as cited in Yuszu 2016). Therefore, the applied load drops promptly until fracture. Rupture stress/strength is not always the same as ultimate stress/strength, depending on some material factors. Rupture stress is the stress at the time of rupture, but this stress ―is not usually an important quantity for design standpoint", according to Yuszu (2016).

2.5.4 Fracture stress

After necking, plastic deformation is not uniform and the stress decreases accordingly until fracture. The fracture strength (σ fracture) can be calculated from the load at fracture divided by the original cross-sectional area, Ao, as expressed in Eq. (2.4).

$$\sigma_{fracture} = \frac{P_{fracture}}{A_o} \qquad\qquad (2.4)$$

2.5.5 Fracture Strain, σf

After necking, plastic deformation is not uniform and the stress decreases accordingly until fracture. The fracture strength (σ fracture) can be calculated from the load at fracture divided by the original cross-sectional area, Ao, as expressed in Eq. (2.5)

$$\sigma_{fracture} = \frac{\sigma_{fracture}}{A_o} \qquad (2.5)$$

2.5.6 Fracture Strain

Figure 2.3, Necking of a tensile specimen occurring prior to fracture

2.5.7 Tensile ductility

Tensile ductility of the specimen can be represented as % elongation or % reduction in area as expressed in the Eqs. (2.6) and (2.7)

$$\%Elongation = \frac{\Delta_L}{L_o} \times 100 \qquad (2.6)$$

$$\%RA = \frac{A_o - A_f}{A_o} \times 100 \qquad (2.7)$$

where

A_f is the cross-sectional area of specimen at fracture.

The fracture strain of the specimen can be obtained by drawing a straight line starting at the fracture point of the stress-strain curve parallel to the slope in the linear relation. The interception of the parallel line at the x axis indicates the fracture strain of the specimen being tested.

2.5.8 Young modulus

During elastic deformation, the engineering stress-strain relationship follows the Hook's Law and the slope of the curve indicates the Young's modulus (E) as in Eq. (2.8).

$$E = \frac{\sigma}{\varepsilon} \qquad (2.8)$$

Apart from tensile parameters mentioned previously, analysis of the area under the stress strain curve can give informative on material behavior and properties. By considering the area under the stress-strain curve in the elastic region (triangular area) as illustrated in figure 2.3, this area represents the stored elastic energy or resilience. The latter is the ability of the materials to store elastic energy which is measured as a modulus of resilience, UR, as follow, Eq. (2.9):

$$U_R = \frac{\sigma_o \varepsilon_o}{2} = \frac{\sigma_o^2}{2E} \qquad (2.9)$$

The significance of this parameter is considered by looking at the application of mechanical springs which requires high yield stress and low Young's modulus. For example, high carbon spring steel has the modulus of resilience of 2250 kPa while that of medium carbon steel is only 232 kPa.

Young's modulus is of importance where deflection of materials is critical for the required engineering applications. This is for examples: deflection in structural beams is considered to be crucial for the design in engineering components or structures such as bridges, building, ships, etc. The applications of tennis racket and golf club also require specific values of spring constants or Young's modulus values (Callister, 2001).

19

2.6 Deformation and fracture characteristics of mild steel pipes

Sklenicka et al. (2015) investigated the creep behavior of thick walled P92 steel pipe bent (90°) using local induction heating at 600 and 650°C. They studied uniaxial tension creep test to provide detailed information on the creep behavior. They showed that, irrespective of the bend position, hot bending of the pipe decreases the creep resistance compared to the unbent pipe. There was similar creep rupture strength at intrados and extrados, even the extrados region of bend offered higher creep resistance and longer time to fracture.

Sellakumar et. al. (2013) investigated the impact of high piping stress on operating piping systems which can be dramatic and costly. Yet for many piping designers, piping stress analysis is the least – understood area of pipe knowledge. A thoroughly analyzed plant will last longer and be more cost effective. Neglecting the impact of the weight of the pipe and thermal expansion of hot pipe can cause significant maintenance problem due to high piping stress as the following: Pump bearings worn-out, Cracks developing in vessel and nozzle junctures, Flanges leaking flammable liquids and Pipe permanently deforming.

He et al. (2012) investigated the analysis of bending characteristics and multiple defects, advances on exploring the common issues in tube bending are summarized regarding wrinkling at the intrados, wall thinning at the extrados, spring-back phenomenon, cross-section deformation.

Wen (2014) proposed a new concept of rotary draw bending die called Multiple Diameter Bending-Die, on which tubes with different outer diameters can be bent by adjusting the thickness of pads and then changing the shape of the die groove. They also studied the deformation of tubes with different outer diameters, wall thickness,

and bending angles when bent on the Multiple Diameter Bending-Die by experimental methods.

2.7 Chapter Summary

From the literature, the most commonly experimental test method used to analysed the effect of loading on the mechanical properties of mild steel pipes is tensile test experiment. So, by implication the study would use tensile test experiment to arrive at the process leading to deformation and fracture characteristics of mild steel pipes. AISI 1018 mild steel and ASTM A36 mild steel are discussed in the literature, but AISI 1018 mild steel is the sample used in the experiment.

In effect the study compares the effect of load on the mechanical properties of both bent and welded curve square pipes. Therefore, this study focused on the use of tensile test experiment to arrive at the process leading to deformation and fracture characteristics of mild steel pipes.
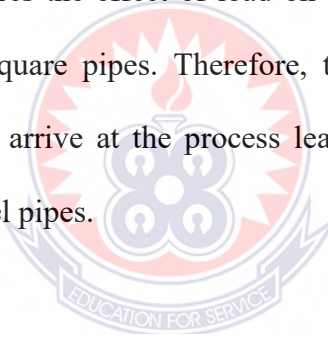
CHAPTER THREE

RESEARCH METHODOLOGY

3.1 Introduction

This chapter presents the tools, equipment and the methods (procedures) used for the study which includes preparation of samples, mechanical (tensile) testing of the samples as well as the impact analysis of the samples. Preparation of the samples was done at the Akenten Appiah-Minkah University of Skills Training and Entrepreneurial Development (Aamusted) Mechanical and Automotive Technology workshop in Kumasi, using the shearing machine, an Arc welder and square pipe bender.

3.2 Materials and Methods

The samples specimen used for the study is 25mm AISI 1018 mild Steel square pipe. Straight square pipe, Bent square pipes as well as curved welded samples were prepared from the AISI 1018 mild steel material which has carbon content of 0.5500%. Other major elements present in this steel material are; Manganese (0.7500%), Sulphur (0.0500%) Phosphorus (0.0400%). The mechanical tests were conducted at Aamusted. Standard mechanical tests laboratory using bent, welded and unwelded mild Steel square pipes. Accordingly, the following machines and equipment were used for the study; Standard Universal Tensile Test Machine embedded with FESSLIX software (for tensile test analyses), and a Microsoft excel 2010 for generating graphs and charts. Also the metallurgraphical examination method was used for micro-structural analysis.
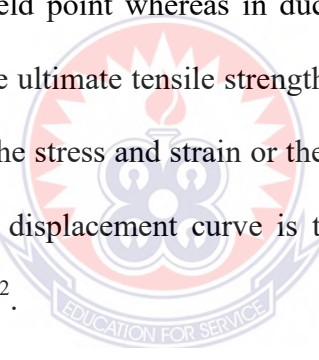
Data obtained from the study was analysed using graphs, tables and charts. The computer-interfaced tensile test machine, solid works and MATLAB 2016 was used to plot, the load-displacement graphs for the various sets of sample specimen.

Before performing the experiment, the sample preparation of the pipes needed to be developed at welding workshop and the lab by using basic workshop tools and machines. Also the SOLIDWORKS software aided in modelling the square pipes and simulation of the impact test analysis. The process made it possible to compare the different specimen results.

3.3 Mechanical Properties

3.3.1 Ultimate Tensile Strength (UTS)

The Ultimate Tensile Strength of a material is the maximum tensile stress that the material can withstand without failing. In brittle materials, the ultimate tensile strength is close to the yield point whereas in ductile materials the ultimate tensile strength can be higher. The ultimate tensile strength is usually found by performing a tensile test and recording the stress and strain or the load displacement produced. The highest point on the load displacement curve is the ultimate tensile strength. It is measured in Pascal or N/m^2.

3.3.2 Yield Strength

The Yield Strength of a material is the maximum stress that the material can withstand before permanent deformation occurs. The yield point is the point on the stress-strain curve that indicates the limit of elastic behavior and the beginning of plastic behavior. The yield strength is often used to determine the maximum allowable load in a mechanical component, since it represents the upper limit to which forces that can be applied without producing permanent deformation. It is measured in Pascal or N/m^2.

3.3.3 Stress

When a specimen is subjected to an external tensile loading, the metal will undergo elastic and plastic deformation. Initially, the metal will elastically deform giving a linear relationship of load and extension. These two parameters are then used for the calculation of the engineering stress and engineering strain to give a relationship as follows in Eqs. (3.1) and (3.2)

$$\sigma = \frac{P}{A_o}$$

(3.1)

$$\varepsilon = \frac{L_f - L_o}{L_o} = \frac{\Delta L}{L_o}$$
(3.2)

where

σ is the engineering stress

ε is the engineering strain

P is the external axial tensile load

Ao is the original cross-sectional area of the specimen

Lo is the original length of the specimen

Lf is the final length of the specimen

The unit of the engineering stress is Pascal (Pa) or N/m according to the SI Metric Unit whereas the unit of psi (pound per square inch) can also be used. ―It is desirable to plot the data, results of tensile testing, of the stress-strain curve if the results are to be used to predict how a metal will behave under other forms of loading" ASTM International (2004). Stress-strain curve is the output of tensile testing and it describes two important concepts: mechanics of materials and mechanics of deformable bodies. The stress-strain is usually plotted as load/force corresponding to elongation, with the

24

stress along the y-axis and the strain along the x-axis. The nominal stress is defined as Eq. (3.3) and strain as in Eq. (3.4)

$$\sigma = \frac{P}{A_o}$$

(3.3)

$$\varepsilon = \frac{L_f - L_o}{L_o} = \frac{\Delta L}{L_o}$$ (3.4)

The basic curve can be divided into two regions: elastic and plastic. In basic engineering design, the material starts in linear elastic region. In the elastic region, the tensile stress is proportional to the strain with the constant of proportionality, and the stress-strain curve is linear Eq. (3.5).

$$\sigma = E\varepsilon$$ (3.5)

3.3.4 Strain

The Strain of a material is the elongation or the increase in length of the material when subjected to tensile stress. It is a description of deformation in terms of the relative displacement of particles in the body that excludes rigid-body motions. Deformations, which are recovered after the stress has been removed, are called elastic deformations. .

3.3.5 Elastic (Young's) Modulus

It is a measure of the stiffness of a material; it defines the relationship between stress (force per unit area) and strain (proportional deformation) in a material. The slope of a stress- strain curve represents the elastic modulus of the material. The relationship between stress and strain is described by Hooke's law which states that stress is proportional to strain, provided the elastic limit of the material is not exceeded. The

25

coefficient of proportionality is Young's modulus. The higher the modulus, the more stress needed to create the same amount of strain.

3.4 Preparation of Tensile Test Samples

3.4.1. Specimen Materials

Mild steel is predominant pipe material widely used by both local artisanal welders and engineers. Among various types of mild steel, AISI 1018 mild steel and ASTM 36 mild steel are perhaps the most widely used pipe materials. Because of this, it is reasonable to select one of these two types of materials for load endurance investigation due to their wide use and also design needs in the welding industry. Mild steel is ductile and has been widely used in pipe industry due to its comparatively low cost and its greater strength and ductility.

As is well known, the mechanical properties of a metal are affected by its chemical composition, morphology, and microstructure which vary significantly. In this study, AISI 1018 mild steel is selected as the testing materials due to their wide use by welding engineers in design works and also in the pipe industry in Ghana and availability on market.

3.4.2 Specimens for Tensile Strength

Specimens for tensile strength test were prepared to the required specifications using a horizontal band saw machine. Also, the edges of all the samples were grinned to (smoothened) to reduce their edge roughness and shape of standard dimensions, using American Iron and Steel Institute (AISI) standard relation for dimensioning of tensile test sample specimen.

The testing specimens are recommended single-edge bend [SE(B)] in the standard, of which the dimensions should comply with the following requirement:

$L \geq 4D$, where

L is the gauge length and D is the diameter of the middle part of the specimen within gauge length L.

For the sake of comparison, the specimens of the two different materials for tensile strength test are intentionally made with the same dimensions.

Dimension of each of the entire three curve sample specimen (Specimen L)

D= 25.4 mm

d = 24.4 mm

Lo = 609.6 mm

Dimension of each of the entire three bent sample specimen (Specimen C)

D= 25.4 mm

d = 24.4 mm

Lo = 609.6 mm

R= 150 mm

Dimension of each of the entire three straight sample specimens (Specimen S)

D= 25.4 mm

d = 24.4 mm

Lo = 609.6 mm

Figure 3.1 - 3.3; show the shape of welded samples and while figures 3.4 - 3.9 show the geometric of shapes of unwelded samples.

All dimensions are in millimeters.

Electric arc welding was used to weld each of the samples labeled ⊥ shape specimen A".
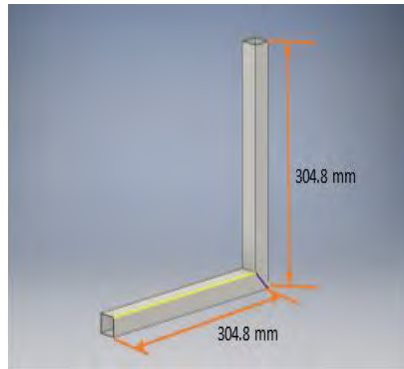
Figure 3.1 Geometric of L shape Specimen 'L1' at a load of 7.35KN

(Source: Lab Work, November, 2020)
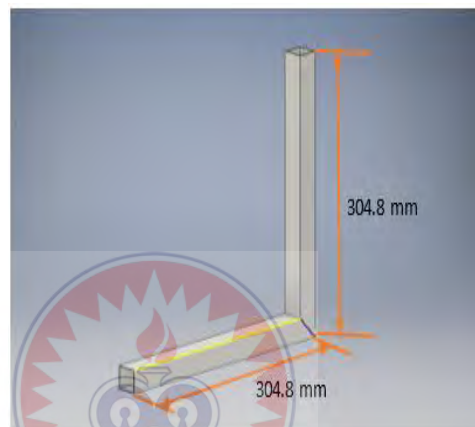
Figure 3.2 Geometric of L shape Specimen 'L2' at a load of 8.5KN

(Source: Lab Work, November, 2020)
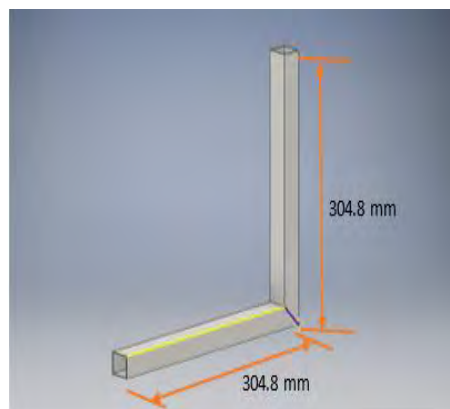
Figure 3.3 Geometric of L shape Specimen 'L3' at a load of 4.55KN

(Source: Lab Work, November, 2020)
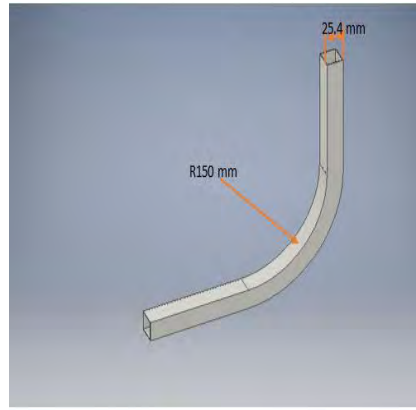
Figure 3.4 Geometric of bent shape (curve shape) Specimen 'C1' at a load of

5.85KN

(Source: Lab Work, November, 2020)
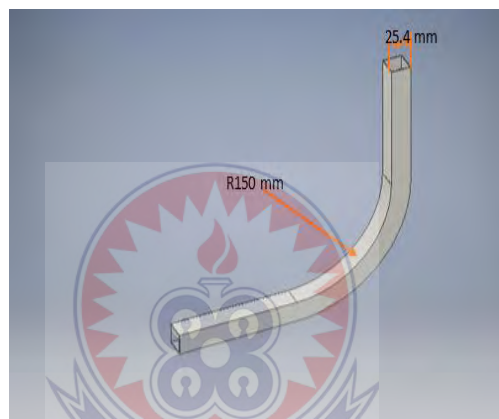
Figure 3.5 Geometric of bent shape (curve shape) Specimen 'C2' at a load of

5.1KN

(Source: Lab Work, November, 2020)
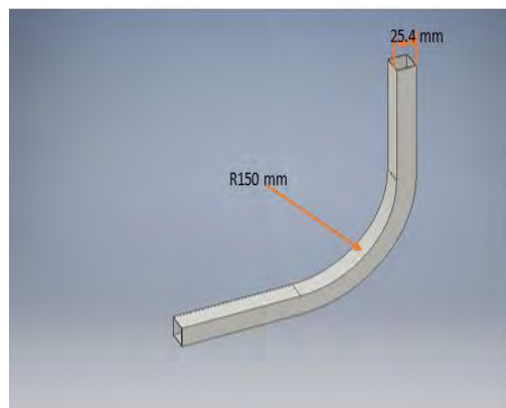
Figure 3.6 Geometric of bent shape (curve shape) Specimen 'C3' at a load of

7.35KN

(Source: Lab Work, November, 2020)

29
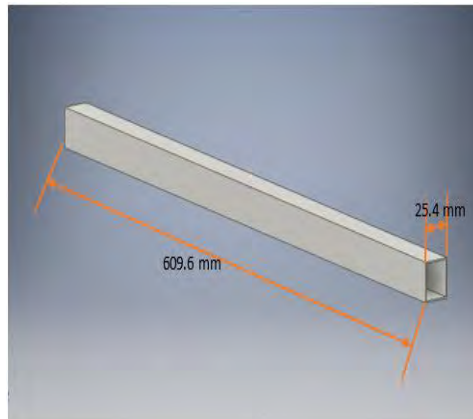
Figure 3.7 Geometric of straight shape Specimen 'S1' at a load of 9.65KN

(Source: Lab Work, November, 2020)
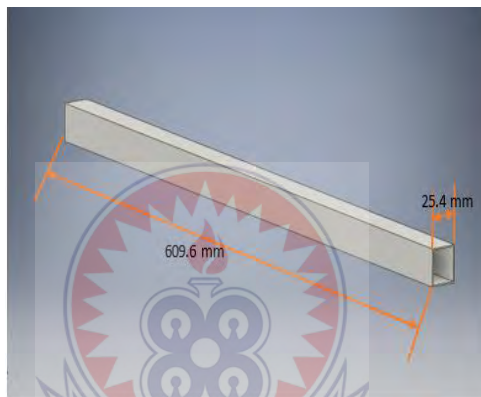
Figure 3.8 Geometric of straight shape Specimen 'S2' at a load of 9.1KN

(Source: Lab Work, November, 2020)
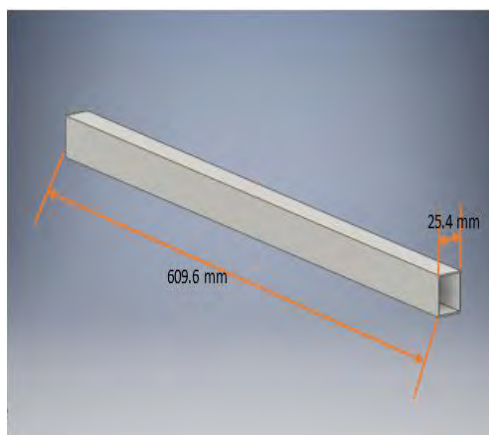
Figure 3.9 Geometric of straight shape Specimen 'S3' at a load of 8.45KN

(Source: Lab Work, November, 2020)

3.4.3 Welded sample

Figure 3.10 show welded samples of curve shape Specimen. The welded samples were also prepared according to the AISI standard for welded tensile test specifications, with the same dimensions as the unwelded samples. The samples were cut to standard dimension and beveled weld, to ensure good weld is achieved. Electric arc welding (with standard 6013 mild steel welding electrode) was used to weld the sample specimen, and later normalized in ‒still air" in order to relieve the thermal stresses that may have been induced at the heat affected zone (HAZ) during the welding processes. A pyrometer was used to read the annealing and normalizing temperatures.

Figure 3.10 Prepared Welded samples of curve shape Specimen for tensile test (Specimen A)
(Source: Lab Work, November, 2020)

3.4.4 Bent sample

Figure 3.11 show bent samples shape Specimen. The bent samples were also prepared according to the AISI standard for bent tensile test specifications, with the same dimensions as the welded samples. The samples were cut to standard dimension using the horizontal band saw cutting machine for hollow sections to achieve the desired

dimensions. The edges were smoothened. A tape measure was used to check the required dimensions.

Figure 3.11 Prepared Bent sample shape Specimen for tensile test (Specimen B)

(Source: Lab Work, November, 2020)

3.4.5 Straight sample

Figure 3.12 show straight samples shape Specimen. The straight shape samples were also prepared according to the AISI standard for mild steel pipes tensile test specifications, with the same dimensions as the welded samples. The samples were cut to standard dimension using the horizontal band saw cutting machine for hollow sections to achieve the desired dimensions. The edges were smoothened by grinding. A tape measure was used to check the required dimensions.

Figure 3.12 Prepared Straight sample shape Specimen (Specimen C)

(Source: Lab Work, November, 2020)

3.5 Tensile Test Procedure

Each of the tensile test samples specimen was placed in the computerized universal testing machine, with an extensometer connected to it. One end of the specimen was secured firmly to the non-movable jaw by means of a fixture while the other end was secured in the movable jaw of the universal tensile testing machine with another fixture. The average temperature of the samples was 38 ˚C.

The load control knob (actuator) was subsequently activated to apply a constant speed and a steady tensile load to each of the specimen until the specimen failed. Consequently, the curve shape specimen, the bent shape specimen and the straight shape specimen failed at the welded joint, bent region and the mid portion respectively. Some failed specimens are shown in Figures 3.13. With the aid of the load sensor attached to the test specimen, the increasing tensile stresses, load and displacement were measured digitally. The extensometer recorded the corresponding changes in the length of the test specimen arising from the application of the tensile loads. With the aid of the computer monitor (embedded with FESSLIX software) connected to the testing machine, the load displacement graphs were generated for each three set of samples under each shape of the test specimens using a Computerized universal tensile machine as shown in Fig. 3.14

Figure 3.13 failed curve welded shape specimen

(Source: Lab Work, November, 2020)

33

Figure 3.14 Computerized Universal Tensile Test Machine

(Source: Lab Work, November, 2020)

3.6 Preparation of Impact Test Simulation

The impact test method is used to conduct the impact analysis of the square mild steel pipe for curved and bends shapes samples. SOLIDWORKS software is used to model the three samples each of an AISI 1018 mild steel pipe with straight pipes of length 25mm pipe's outer diameter (L = 25D) as shown in figure 3.15. The average size of the mesh is chosen to be 15x15 mm since the model is simple and is not time consuming. A linear material is used to define the pipe behaviour where the Young's modulus of elasticity is 205000 N/mm^2 and Poisson's ratio is 0.29. An end rotational displacement of 0.1 radians is applied at the free end of the pipe. The displacement is applied in an increment of 0.025 radians. Nonlinear geometry is considered in the analysis to account for the cross-sectional deformations as well as the overall deformation of the pipe. The Von Mises, hoop and longitudinal stresses are obtained from the SOLIDWORKS numerical models at the location of critical stresses. These stresses are measured at the outer, inner and mid-layer of the pipe wall thickness. The stresses from the SOLIDWORKS models are later compared.

(a) Impact test model for L- Shape sample

(b)Impact test model for C- Shape sample

(c)Impact test model for S- Shape sample
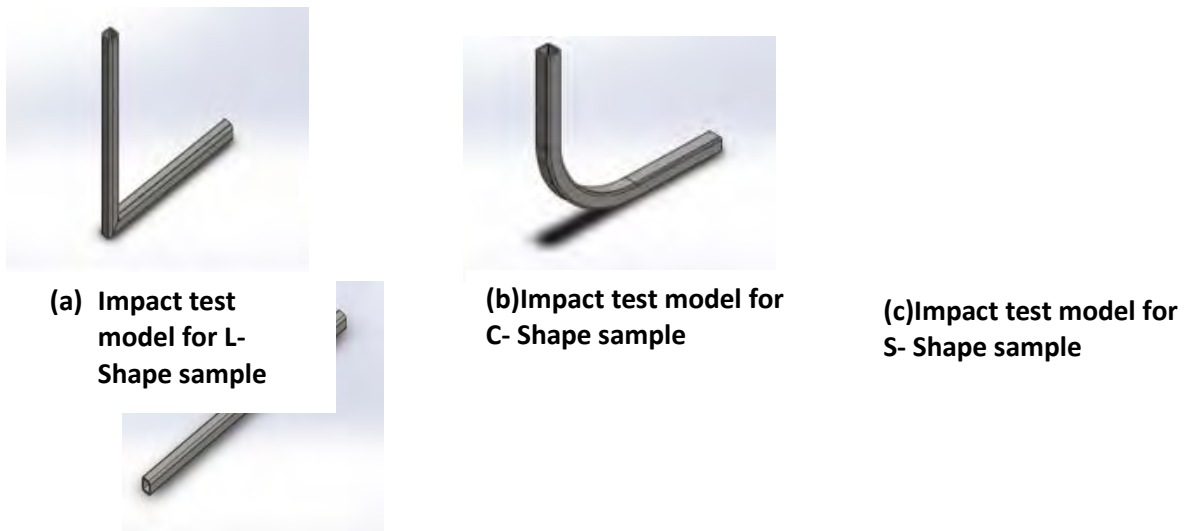
Figure 3.15 Impact test model for L, C and S Shape Samples

3.6.1 Simulation Procedure

The solidworks 2017 software icon was clicked on the desktop menu on the window interface and new part was clicked on followed by clicking on the sketch tab which activated all the design tools which were used to design the sample specimen shown in Figure 3.16.
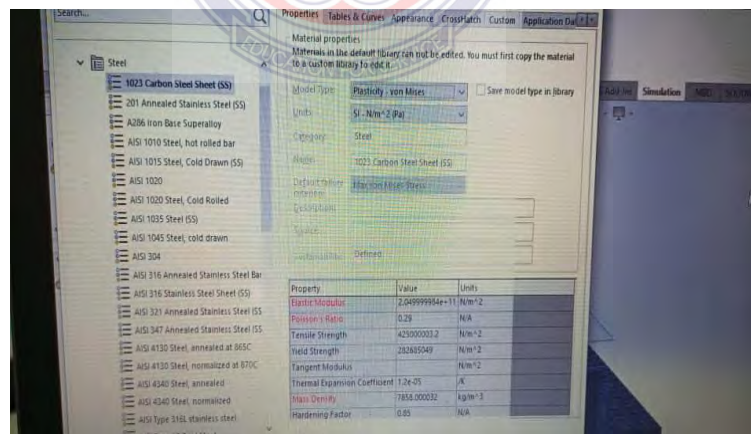
Figure 3.16 Design interface for solid works Simulation

After the completion of the design of each: L-Shape, Bent shape and the straight shape samples, exit sketch was clicked on the window interface and design tools were deactivated. The simulation tab was checked and all the tools required for simulation were activated and displayed. The wizard option was clicked on to activate a pop-up

35

window. A new project option was clicked on and selection of simulation parameters were displayed. Material Properties (Specimen name, model type, default failure criterion, Yield strength, Tensile strength, Elastic modulus Poisson's ratio, Mass density, shear modulus etc), Units, Loads and fixtures, mesh information, analysis type and finish icon were clicked on and the computational domain was automatically created around the design. Prior to running the simulation, the computational domain, boundary conditions and global goals were selected after which the run icon on the window interface was clicked on. The simulation results were generated for the L-specimen, Bent specimen and straight sample specimen respectively.

3.7 Microstructural Tests

The microstructure of steel gives the appearance of the etched surface viewed under a microscope or a magnifying glass. Etching involves rushing or stirring a metal through a strong acid to enhance its micrographic view under a microscope. Each of the test sample specimens under study were prepared by first fine-grinding (polishing) their surfaces. The polishing was done to ensure a uniform surface finish. The test specimens were etched with a 3% nitrite acid, with the remaining 97% being alcohol, for about 20 seconds. The surfaces were then cleaned and completely dried in the open air. After completely drying the test samples, the specimens were placed under a 100X Aven microscope for microscopic analyses.

CHAPTER FOUR

RESULTS AND DISCUSSION

4.1 Introduction

This chapter presents the results and discussion of the study. The results are presented in order of the procedure adopted for the study; the bent mild steel pipe results, the welded mild steel pipe results, the analysis of the mechanical properties of the bent and welded mild steel pipes results and the comparison of the deformation and fracture characteristics of bent and welded mild steel pipes results. The tensile test results were used for the analysis. The test results were obtained from the load-displacement/stress-strain graphs generated by the Excel software embedded in the computer monitor.

4.2 Welded Mild Steel Pipe Results

4.2.1 Ultimate Tensile Strength (UTS) of Samples Specimen 'L' (welded mild steel pipe)

The tensile test results for specimen ⌐L' are presented in Table 4.1 and Figure 4.1.

Table 4.1 Mechanical Properties of Specimen 'L'

Sample	Area mm^2	Load kN	UTS N/mm^2	Modulus Elasticity GPa	Strain %
L1	88	7.35	83.523	74	0.113
L2	88	8.5	96.591	74	0.131
Average	**88**	**6.8**	**77.273**	**74.000**	**0.104**

KEY: L1 - Shape Welded Sample at 7.35KN   :   L2 - Shape Welded Sample at 8.5KN

Figure 4.1: Load - Displacement for Specimen 'L' at different loading conditions
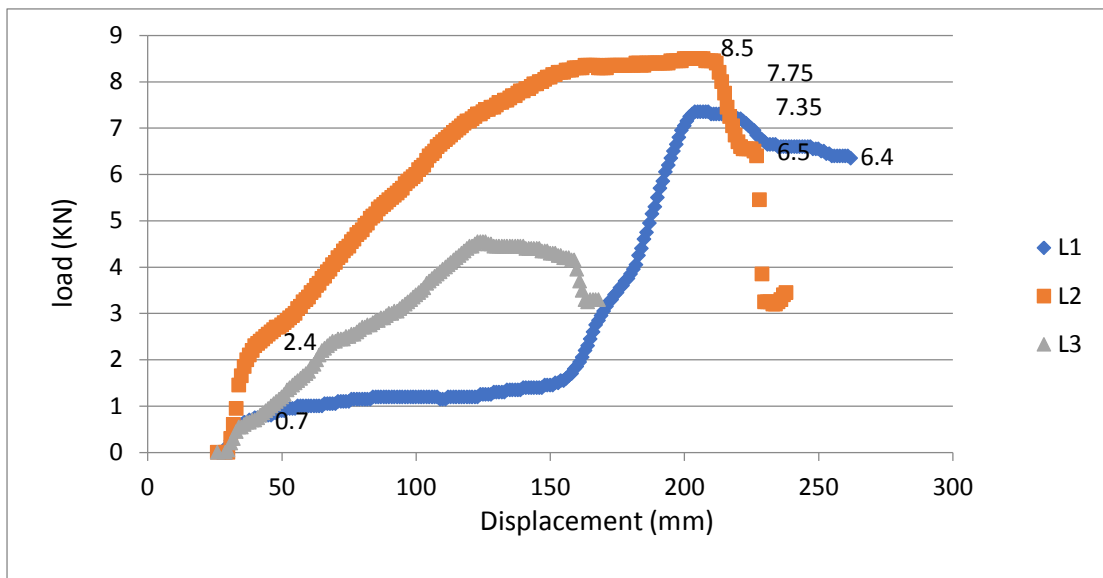
From Table 4.1 and Figure 4.1, the Ultimate Tensile Strength (UTS) of Specimen _L1' and Specimen _L2' of the welded L-Shaped specimen are 83.523 MPa, and 96.591 MPa respectively, indicating an increase of 13.068 MPa in the UTS of the sample. This represents an increase of 15.65% of the initial UTS value of 83.523MPa. This means that an increase in load will lead to a higher UTS value of the L - shape sample. The implication is that, the welding has increase it brittleness making the sample harder and more stressed as the load is exerted on it.

4.2.2 Yield Strength of Samples Specimen 'L' (welded mild steel pipe)

From Table 4.1 and Figure 4.1, the load at Yield Point of Specimen _L1' and Specimen _L2' of the welded L-Shaped specimen are 7.35KN, and 8.5KN respectively, indicating an increase of 1.15KN in the Yield Point load. This represents a percentage increase of 15.65%. This implies that as more load is applied, the material will be more stressed and more likely to fail more beyond that point.

38

4.2.3 Elastic Modulus

From Table 4.1 and Figure 4.1, the Elastic Moduli of Specimen ‗L1' at a load of 7.35 KN is 74GPa and the Elastic Moduli of Specimen ‗L2' at a load of 8.5 was 74GPa. This indicates that a marginal increased in Load does not cause an increase in the elastic modulus of Specimen L due to the weld.

4.2.4 Percentage Strain in Specimen

From Table 4.1 and Figure 4.1, the percentage strain of Specimen ‗L1' at a load of 7.35 KN is 0.113% and the percentage strain of Specimen ‗L2' at a load of 8.5 was 0.131%, implying an improvement of 0.018%. This means that, the welding process induces more stresses on the sample specimen ‗L2' which make the sample less strain and does not stretch wide.

4.3 Bent Mild Steel Pipe Results

4.3.1 Ultimate Tensile Strength (UTS) of Sample 'C1' Specimen

The tensile test results for specimen ‗C' are presented in Table 4.2 and Figure 4.2.

Table 4.2 Mechanical Properties of Specimen 'C'

Sample	Area mm^2	Load KN	UTS N/mm^2	Modulus Elasticity GPa	Strain %
C1	88	5.85	66.477	13	0.511
C2	88	5.1	57.955	85	0.068
Average	**88**	**5.475**	**62.216**	**49.0**	**0.545**

KEY: C1 - Shape Bent Sample at 5.85KN : C2 - Shape Bent Sample at 5.1KN

39
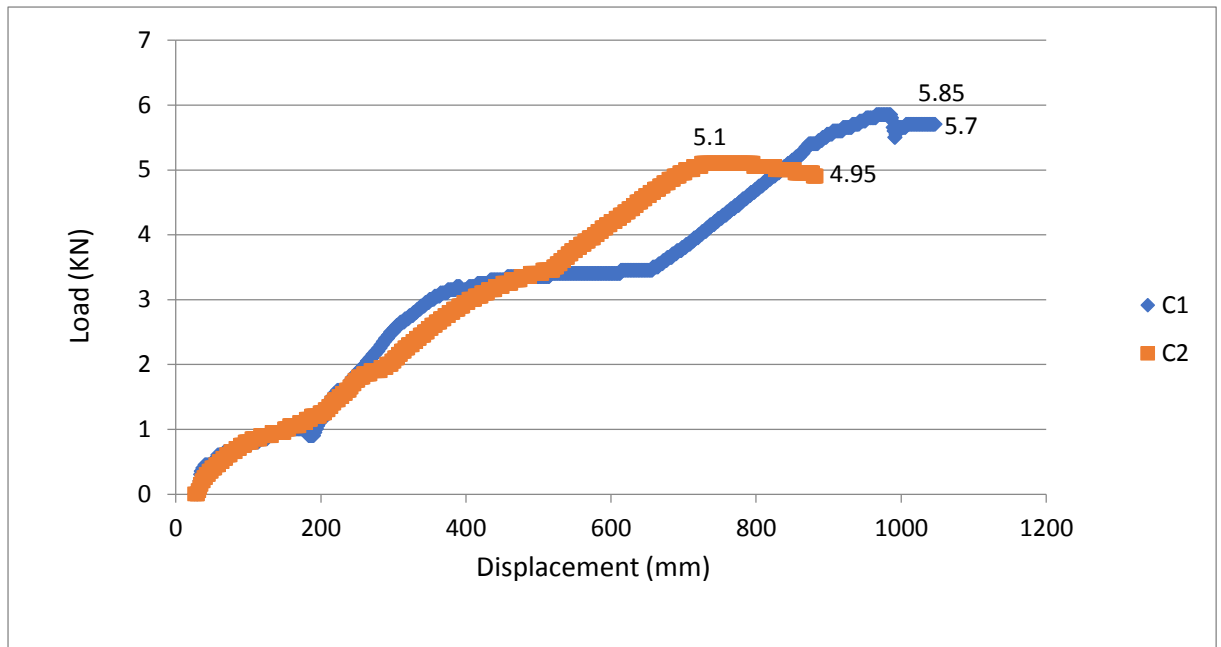
Figure 4.2: Load - Displacement for Bent shape Specimen ‗C' at different loading conditions

From Table 4.2 and Figure 4.2, the Ultimate Tensile Strength (UTS) of Specimen ‗C1' when a load of 5.85KN was applied on the bent shaped Specimen is 66.477 MPa. When the load was reduced to 5.1KN, the (UTS) value of sample ‗C2' also reduced to 57.955 MPa, indicating a percentage drop of 14.70%. The implication of this result is that the material is Tough but Ductile and soft and can stretch wide.

4.3.2 Yield Strength of Sample Specimen 'C'

From Table 4.2 and Figure 4.2, the load at Yield Point of Specimen ‗C1' and Specimen ‗C2' of the bent Shaped specimen are 5.85KN, and 5.1KN respectively. This represents a reduction of 0.75KN and a percentage drop 12.82% of the initial load applied. This shows that bending has made the sample strain and has negatively affected the Yield strength of the sample.

4.3.3 Elastic modulus of Sample Specimen 'C'

From Table 4.2 and Figure 4.2, the Elastic Moduli of Specimen ‗C1‗at a load of 5.85 KN is 13GPa and the Elastic Moduli of Specimen ‗C2‗ at a load of 5.1 was 85GPa. This implies that the elastic modulus of specimen reduced slightly by 0.75GPa, indicating a percentage increase of 84.71%.

4.3.4 Percentage Strain in Specimen 'C'

From Table 4.2 and Figure 4.2, the percentage strain of bent samples ‗Cl‗ and bent Samples ‗C2‗ are 0.511% and 0.068% respectively. This represents a reduction of 0.443%, implying the variations in load application has affected the percentage strain of the specimen.

4.4 Analysis of the mechanical Properties of Bent and Welded Mild Steel Pipes Results

The mechanical properties of the bent and welded mild pipes that are displayed on the load-displacement graph are the ultimate tensile strength, yield strength, Young's Modulus and fracture stress when the two were separately subjected to uniaxial tensile loading.

4.4.1 Ultimate Tensile Strength (UTS) of Samples Specimen

The tensile test results for combined specimen ‗L‗ and ‗C‗ are presented in Table 4.3 and Figure 4.3

Table 4.3 Combined Mechanical Properties of Specimen 'L' and 'C'

Sample	Area	Load	UTS N/mm^2	Modulus	Elasticity	Strain
	mm^2	kN		GPa		%
L	88	6.8	77.273	74		0.511
C	88	5.475	62.216	49.0		0.068

**KEY: L – Welded Shape Sample : C - Bent Shape Sample**
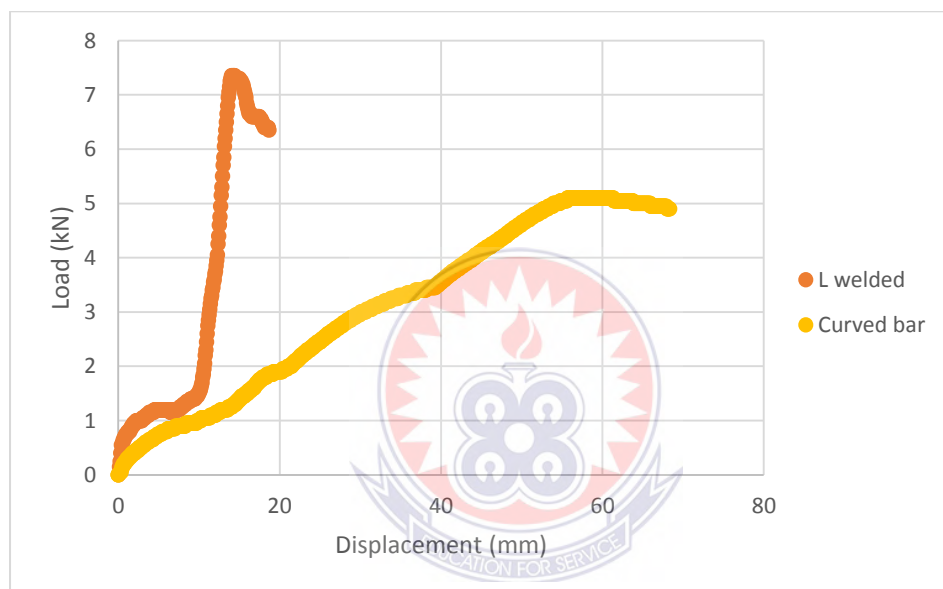
Figure 4.3 Load - Displacement for Welded and Bent shape Specimen at different loading conditions.

From Table 4.3 and Figure 4.3, the Ultimate Tensile Strength (UTS) of Specimen ‗L' and Specimen ‗C' of the welded L-Shaped specimen and the bent C -Shape Specimen are 77.273 MPa, and 62.216 MPa respectively, indicating a reduction of 15.057 MPa in the UTS of the sample L. This represents a drop 19.485% of the initial welded sample UTS value of 77.273MPa. This means that the welding process has resulted in making the L – shape sample more Brittle and harder and will required a higher load to fail and hence a higher UTS value of the L - shape sample. Also, the curve shape

sample C, was ductile and soft which make the C – Shape sample to stretch more and hence lower UTS value.

A summary of the changes in the Ultimate Tensile Strength (UTS) of the tensile test Samples specimen 'L' and 'C' are in indicated in bars in Figure 4.4
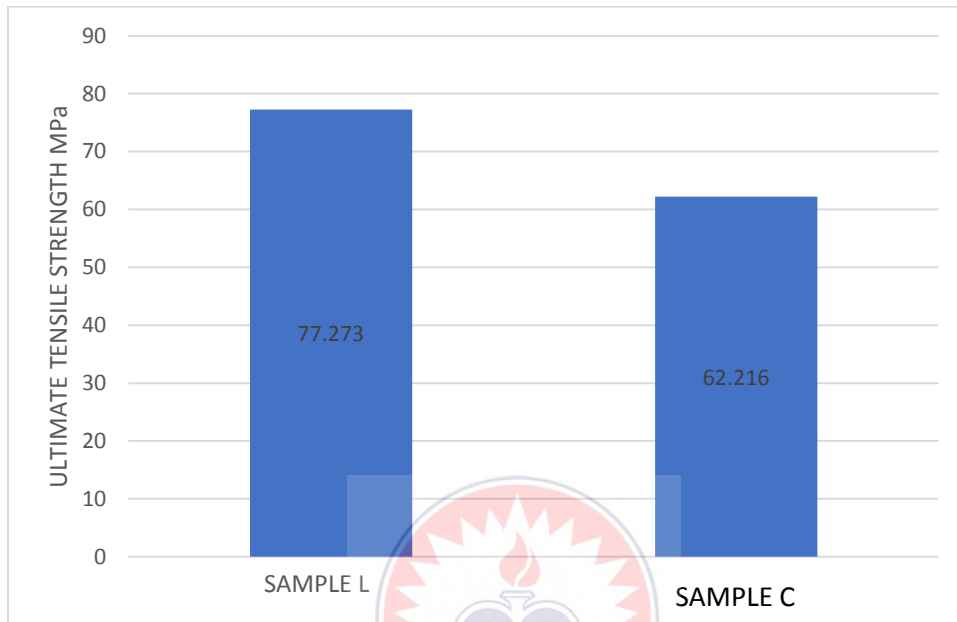
Figure 4.4: Ultimate Tensile Strength (UTS) of Specimen 'L' and 'C'

4.4.2 Yield Strength of Samples Specimen:

From Table 4.3 and Figure 4.3, the load at Yield Point of Specimen ‗L' and Specimen ‗C' of the welded L-Shaped specimen and the bent C–shape specimen are 6.8KN, and 5.475KN respectively, indicating a reduction of 1.325KN in the load Yield Point of the L-shape sample. This represents a percentage drop 19.48% of the welded sample, an indication that, the process of welding has resulted in increasing the brittleness of the welded sample thereby increasing the yield load and Yield Strength of the Specimen L.

A summary of the changes in the Yield Strength (UTS) of the tensile test samples specimen are indicated in the bar charts in Figure 4.5
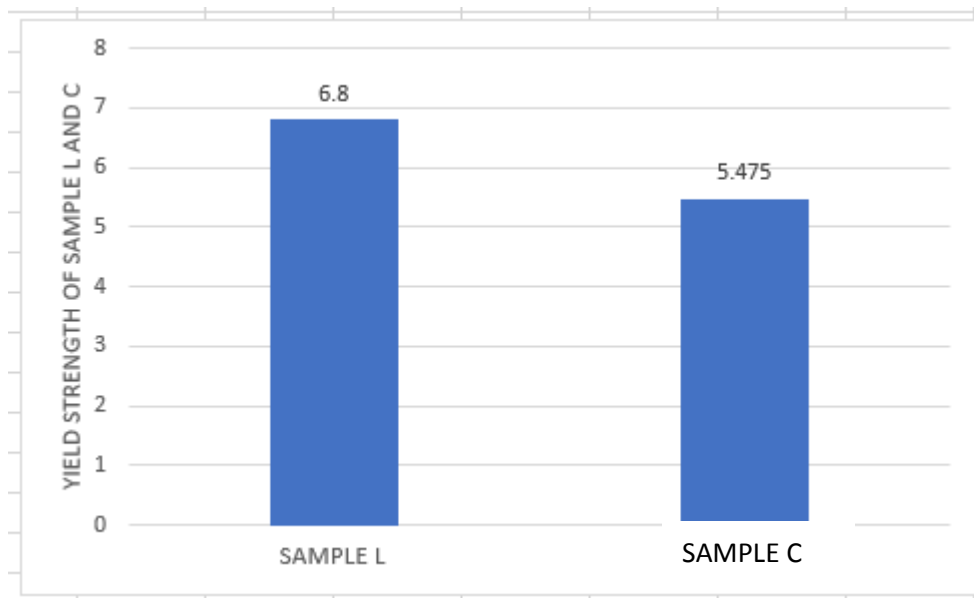
Figure 4.5: Yield Strength of Specimen 'L' and 'C'

4.4.3 Elastic Modulus of Samples Specimen:

From Table 4.3 and Figure 4.3, the Elastic Moduli of Specimen ‗L' and Specimen ‗C'
of the welded L-Shaped specimen and the bent C–shape specimen are 75GPa, and
49GPa respectively. This indicates a marginal reduction in the Elastic modulus of
26GPa and a percentage drop 53.06% of the welded sample, an indication that, the
process of welding has given rise to the highest Elastic modulus of the welded
sample.

A summary of the changes in the Elastic modulus of the tensile test samples specimen
are indicated in the bar charts in Figure 4.6
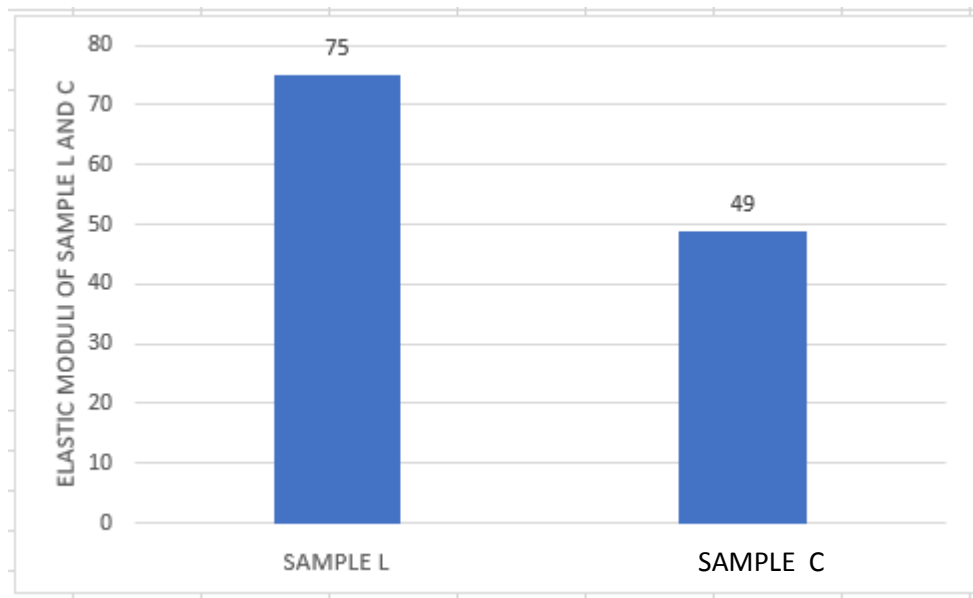
Figure 4.6: Elastic Moduli of Specimen 'L' and 'C'

4.4.3 Percentage Strain in Specimen

From Table 4.3 and Figure 4.3, the percentage strain of Specimen ‗L' at a load of 6.8KN was 0. 511% and the percentage strain of Specimen ‗C' at a load of 5.475 was to 0.068%. This shows that a reduction in load applied adversely affects the percentage strain of about 19.48%.

A summary of the changes in Strain of the tensile test samples specimen is indicated in Figure 4.7
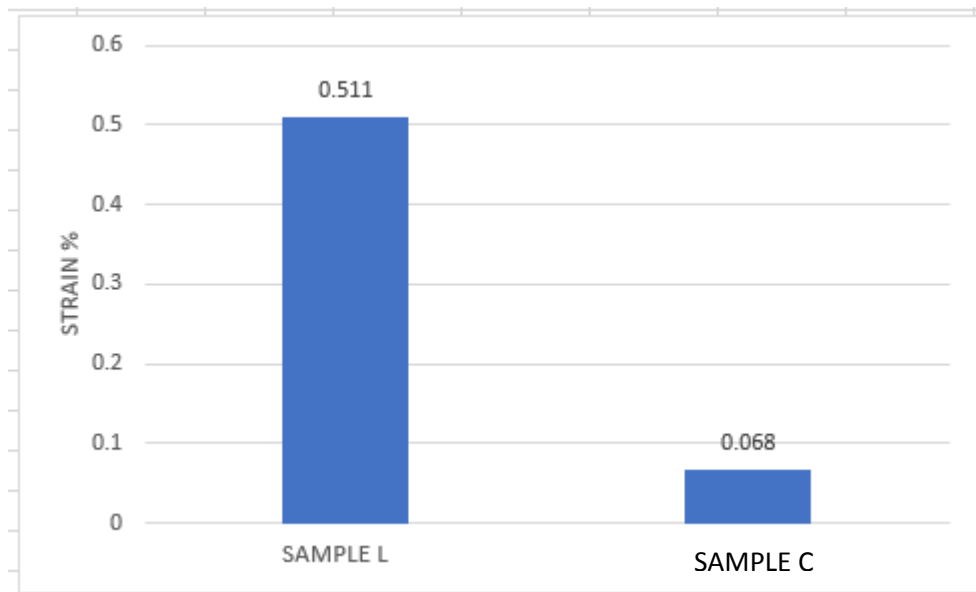
Figure 4.7: Strain (%) of Specimen 'L' and 'C'

4.5 Deformation and Fracture Characteristics of Bent and Welded Mild Steel Pipes.

The deformation and fracture characteristics of the bent and welded mild pipes are obtained from the load – extension graphs, simulation of impact test analysis and microstructure analysis of the bent and welded mild steel pipes. Table 4.4 and Figures 4.8. Stress, Strain and displacement graphs to analyses the deformation characteristics.

4.5.1 Deformation and Fracture Characteristics of bent curve welded shape samples.

The tensile test results for specimen ‗L' and ‗C' are presented in Table 4.6 and figure 4.6

Table 4.4 Deformation and Fracture Characteristics of Specimen 'L' and 'C'

Sample	Area mm^2	Load kN	UTS N/mm^2	Modulus Elasticity GPa	Strain %
L	88	6.8	77.273	74	0.511
C	88	5.475	62.216	49.0	0.068

KEY: L – Welded Shape Sample   :   C - Bent Shape Sample
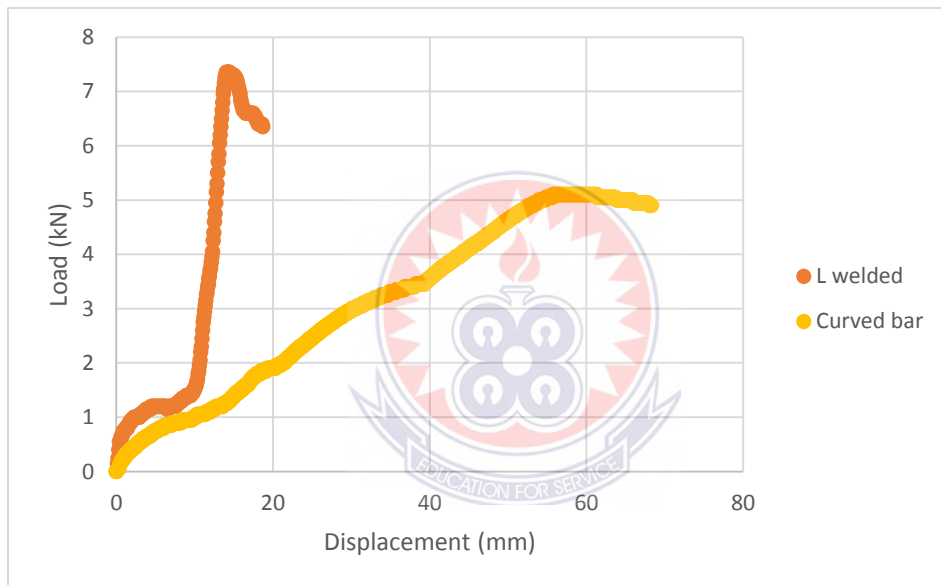
Figure 4.8 Deformation and Fracture Characteristics of Specimen 'L' and 'C'

From Table 4.4 and Figure 4.8, the load applied to specimen ‗L' the welded Sample and specimen ‗C' the bent Sample are 6.8KN and 5.475KN respectively. The load dropped to 1.325KN when bent without welding. This represents a percentage drop of 19.48% of the welding sample, an indication that the welding process induces more stress in the heat affected zone on the sample making it Brittle and harder which will causes the sample to permanently deform at a higher load. On the other hand, the bending process also makes sample ‗C' strain, Tougher and Ductile which make the

47

sample to stretch at a maximum displacement far greater than the L- shape sample. This conforms to available literature by Sklenicka that a marginal increase in displacement as a result of an increase in loads and strain, will leads to an increase in deformation and vice versa.

4.5.2 Impact Test Analysis on the deformation and fracture characteristics

Table 4.5 Impact Test Analysis Specimen L, C and S Shape Sample

DEFORMATION		SPECIMEN	
		L-SHAPE	C-SHAPE
Stress(Von Mises Stress)N/m^2	Minimum	28.0235	10.623
	Maximum	14.338	19.824
Strain	Minimum	20.494	16.737
	Maximum	15.053	27.374
Displacement(mm)	Minimum	0	0
	Maximum	20.821	4.560
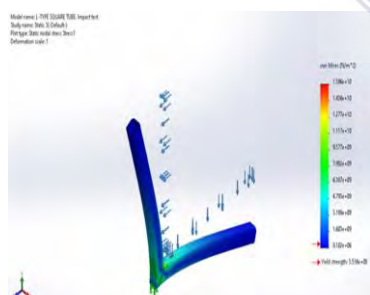
 (a) Stresses Model of Sample 'L'   **(b) Stresses Model of Sample 'C'**
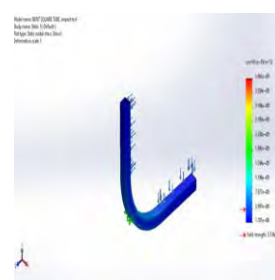
Figure 4.9: Micrographs of Specimen; (a) Bent Sample: (b) Curve Sample

From Table 4.5 and Figure 4.9, the equivalent (Von mises) stress of the ‗L' shape sample and ‗C' shape samples based on distortion energy failure theory, has shown to be particularly effective in the prediction of failure for ductile materials and widely used by designers to check whether their designs will withstand a given load

condition. The tensile test simulation results shows that with the L-shape sample whose welded joint at the centre were held fixed and was subjected to a fixed load, the most stress regions are at the extremes and are more likely to rapture at the ends. Also with the curve shape sample, the most stress region is the curve region and also with the highest stiffness.

(a) Displacement model of sample 'L'   (a) Displacement model of sample 'C'

Figure 4.10: Micrographs of Specimen; (a) Bent Sample: (b) Curve Sample

From Table 4.5. and Figure 4.10., the ‗L' shape sample displaces far from the extreme ends when a fixe load is applied to the sample. The red spots indicate the highest points of displacement and the yellow spots represents the medium spots of displacement, whiles the blue spots represent least displace zone. However in the case of the bent shape sample, during the process of bending the part that was made to move to form the bent also becomes the most stress zone and most displace zone. This will represent the failure region.
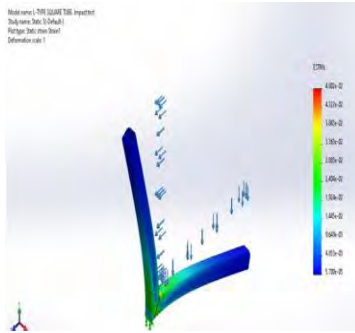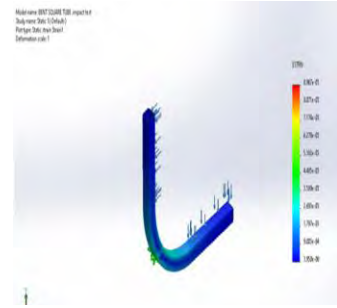
(a) Strain model of 'L'   **(b) Strain model of 'C'**

Figure 4.11: Micrographs of Specimen; (a) Bent Sample: (b) Curve Sample

From Table 4.5.2 and Figure 4.11, the most strain sample is the bent sample. This is because the process only resulted in making the curve zone strain, and the sample becomes more ductile than the welded sample. However, in the case of the l-shape sample, the welding process introduces more carbon into the sample making the sample brittle. This makes sample L requires a larger load to fail or deformed.

4.5.3   Microstructural Assessment
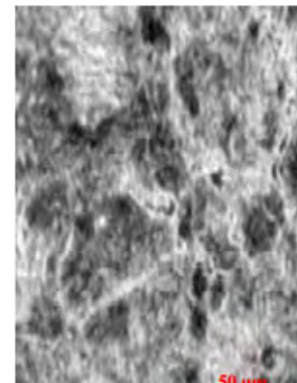
(a) Welded 'L' Sample   **(b) Bent 'C' Sample**

Figure 4.12: Micrographs of Specimen; (a) Bent Sample: (b) Curve Sample

The micrographs of the tensile test sample specimens are presented in Figures 4.5.9. The microstructures of the specimens L-shape are contained in the Micrographs Specimen (a) L - sample after welding and testing. The microstructures of the specimens C-shape are contained in the Micrographs Specimen (b) C - sample after

50

bending and testing. The microstructures were examined under a 100X magnifying power microscope for each samples. The micrographs are mainly made up of pearlites and ferrites. The pearlites are represented in the microstructures by the dark spots whiles the gray spots indicate the ferrites. The average grain size was estimated using ASTM E112 – 12.

As indicated in the micrographs of in both (a) and (b) test samples, the grain size (quantity) of ferrites (grey spots) in the microstructures of the samples, was less than the pearlites (dark spots). However, the grain size (quantity) of ferrites (grey spots) improved significantly in the welded L - samples specimen. The even distribution pattern of the grains (pearlites and ferrites) in the micrographs of the sample specimens after welding, is attributed to the normalizing process carried out to relieve the welded samples of thermal stresses induced during the welding processes and the introduction of additional grains from the welding rod. The improvement in the grain size of ferrites (grey spots) is attributable to the introduction of additional ferrites from the welding electrode into the microstructures of the samples during the welding process and the recrystallization of the grains as a result of the heat treatment (annealing and normalizing) processes. However, there was no improvement in the grain size of ferrites (grey spots) neither there was any introduction of additional ferrites from the cold bending of the pipe into the microstructures of the samples during the bending process.

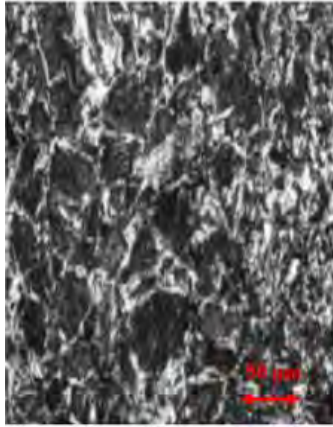(a) ‗C'- Shape Bent Sample   (b) ‗L' - Shape Welded Sample

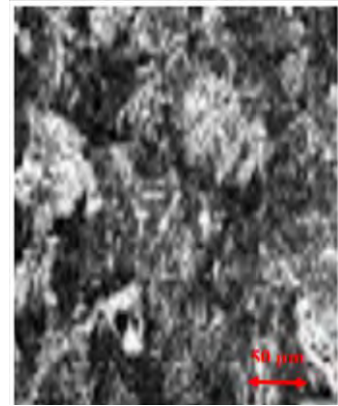**Figure 4.13: Micrographs of Impact Test Specimen; (a) Bent Sample (b) Curve Sample**

The micrographs of the tensile test sample specimens are presented in Figures 4.5.0. The microstructures for the specimens C- Shape is contain in the Micrographs Specimen C – Sample after bending and testing. The microstructures were examined under a 100X magnifying power microscope. Detailed analysis of the microstructure clearly indicated the presence of little dark regions around the bent. These dark sports concentration at the bent region couple with the little – stress within the bent regions let to the formation of due to sudden in increase in dark spots graphs are mainly made up of pearlites and ferrites. The pearlites are represented in the microstructures by the dark spots whiles the gray spots indicate the ferrites. The average grain size was estimated using ASTM E112 – 12.

As indicated in the micrographs the test samples, the grain size (quantity) of ferrites (grey spots) in the microstructures of the samples, was less than the of pearlites (dark spots). However, the grain size (quantity) of ferrites (grey spots) improved significantly after bending the samples specimen C. The even distribution pattern of the grains (pearlites and ferrites) in the micrographs of the sample specimens after bending, is attributed to the bending process carried out on Specimen C.

52

The near even distribution pattern of the grains (pearlites and ferrites) in the micrographs of the sample specimens after welding, is attributed to the normalizing process carried out to relieved the welded sample of thermal stresses induced during the welding processes of Specimen L and the introduction of additional grains from the welding rod. The improvement in the grain size of ferrites (grey spots) is attributable to the introduction of additional ferrites from the welding electrode into the microstructures of the samples during the welding process and the recrystallization of the grains as a result of the heat treatment (annealing and normalizing) processes.

4.5 Summary of Results

From the results and discussion of the welded sample L, it can be observed that;

a) The Ultimate Tensile Strength of specimen L increased by 15.65%.

b) The Yield Strength of specimen L was at a load of 7.35KN.

c) The Elastic Moduli for specimen L increased from a load of 7.35KN to 8.5KN

d) The Percentage Strain for specimen L shape sample increased slightly by 0.018%.

From the results and discussion of the bent sample C, it can be observed that;

a) The Ultimate Tensile Strength of specimen C reduce by 14.70%.

b) The Yield Strength of specimen C reduced by 12.82%.

c) The Elastic Moduli for specimen C reduced from a load of 5.85KN to 5.1KN

d) The Percentage Strain for specimen C reduce slightly by 0.443%.

From the results and discussion of the bent and welded sample L and C respectively:

a) The Ultimate Tensile Strength of specimen L increased over specimen C by 19.48%.

b) The Yield Strength of specimen L increased over specimen C by 19.48%.

c) The Elastic Moduli for specimen L drop from 53.06% below the C sample

d) The Percentage Strain for specimen L shape sample reduce over C shape sample by 19.48%.

From the results and discussion of the deformation and fracture characteristics of bent and welded sample L and C respectively:

Results from tensile testing:

The load applied to specimen ‗L' the welded Sample and specimen ‗C' the bent Sample are 6.8KN and 5.475KN respectively. The load dropped to 1.325KN when bent without welding. This represents a percentage drop of 19.48% of the welding sample, an indication that the welding process induces more stress in the heat affected zone on the sample making it Brittle and harder which will causes the sample to permanently deform at a higher load. On the other hand, the bending process also makes sample ‗C' to be more strain, Tougher and Ductile which make the sample to stretch at a maximum displacement far greater than the L- shape sample.

Results from impact analysis:

(a) The equivalent (Von mises) stress of the ‗L' shape sample and ‗C' shape samples based on distortion energy failure theory. The tensile test simulation results shows that with the L-shape sample whose welded joint at the centre were held fixed and was subjected to a fixed

(b) The ‗L' shape sample displaces far from the extreme ends when a fixe load is applied to the sample. The red spots indicate the highest points of displacement and the yellow spots represents the medium spots of displacement, whiles the blue spots represent least displace zone. However in the case of the bent shape sample, during

the process of bending the part that was made to move to form the bent also becomes the most stress zone and most displace zone.

(c) The most strain sample is the bent sample. This is because the process only resulted in making the curve zone strain, and the sample becomes more ductile than the welded sample. However, in the case of the l-shape sample, the welding process introduces more carbon into the sample making the sample brittle. This makes sample L requires a larger load to fail or deformed

Results from Microstructure analysis:

These results imply that the electric arc welding processes of specimen 'Negatively affected the Ultimate Tensile Strength, Yield Strength and Elastic Moduli of the material studied (i.e. low carbon steel). The results also suggest that low carbon steel specimen components (Specimen ‗C' bent specimens and unbent specimen ‗S') can withstand lower tensile stresses than when the components are welded.

The strain results suggest that the material studied became slightly more Brittle after welding. This can be attributed to the heat induced during the process of welding and bending the sample specimen.

The impact test results suggest that the bent pipe which has low carbon steel components can withstand low impact loads than the welded low carbon steel components. This is largely consistent with available literature, which states that the mechanical properties of a material are internal parameters that do not change substantially unless the properties are purposefully manipulated with external factors such as bending, welding, doping, heat and surface treatment among others. The ferrites (grey spots) distribution in the micrographs of the ‗L' shape welded samples increased remarkably. This can be seen in the near-even distribution of pearlite and ferrite grains in the micrographs of the welded samples specimen. The increase in the

grain size (quantity) of ferrites is attributed to the addition of ferrites from the welding electrode and bending into the microstructures of the samples, during the welding and bending process and the recrystallization of the grains.

The study did not establish a clear-cut relationship between the welded and bent samples, and their Ultimate Tensile and Yield Strengths of both the welded and bent samples.

However, the study established a negative (inverse) relationship between the welded and the bent samples.

CHAPTER FIVE

SUMMARY OF FINDINGS, CONCLUSION AND RECOMMENDATIONS

5.1 Introduction

This chapter presents a summary of the main and significant findings, the conclusion drawn from the findings, as well as the recommendations and suggestions for further research into the study area.

5.2 Summary of Main Findings

A summary of the main findings of the study is presented as follows;

5.2.1 Main Findings for welded sample L

i. The Ultimate Tensile Strength (UTS) of Specimen ‗L1' and Specimen ‗L2' of the welded L-Shaped specimen are 83.523 MPa, and 96.591 MPa respectively, indicating an increase of 13.068 MPa in the UTS of the sample. This represents an increase of 15.65% of the initial UTS value of 83.523MPa. This means that an increase in load will lead to a higher UTS value of the L - shape sample. The implication is that, the welding has increase it brittleness making the sample harder and more stressed as the load is exerted on it.

ii. The load at Yield Point of Specimen ‗L1' and Specimen ‗L2' of the welded L-Shaped specimen are 7.35KN, and 8.5KN respectively, indicating an increase of 1.15KN in the Yield Point load. This represents a percentage increase of 15.65%. This implies that as more load is applied, the material will be more stressed and more likely to fail more beyond that point.

iii. The Elastic Moduli of Specimen ‗L1' at a load of 7.35 KN is 74GPa and the Elastic Moduli of Specimen ‗L2' at a load of 8.5 was 74GPa. This indicates that a

57

marginal increased in Load does not cause an increase in the elastic modulus of Specimen L due to the weld.

iv. The percentage strain of Specimen ‗L1' at a load of 7.35 KN is 0.113% and the percentage strain of Specimen ‗L2' at a load of 8.5 was 0.131%, implying an improvement of 0.018%. This means that, the welding process induces more stresses on the sample specimen ‗L2' which make the sample less strain and does not stretch wide.

5.2.2 Main Findings for bent sample C

i. The Ultimate Tensile Strength (UTS) of Specimen ‗C1'when a load of 5.85KN was applied on the bent shaped Specimen is 66.477 MPa. When the load was reduced to 5.1KN, the (UTS) value of sample ‗C2' also reduced to 57.955 MPa, indicating a percentage drop of 14.70%. The implication of this result is that the material is Tough but Ductile and soft and can stretch wide

ii. The load at Yield Point of Specimen ‗C1' and Specimen ‗C2' of the bent Shaped specimen are 5.85KN, and 5.1KN respectively. This represents a reduction of 0.75KN and a percentage drop 12.82% of the initial load applied. This shows that bending has made the sample strain and has negatively affected the Yield strength of the sample.

iii. The Elastic Moduli of Specimen ‗C1' at a load of 5.85 KN is 13GPa and the Elastic Moduli of Specimen ‗C2' at a load of 5.1 was 85GPa. This implies that the elastic modulus of specimen reduced slightly by 0.75GPa, indicating a percentage reduction of 84.71%.

iv. The percentage strain of bent samples ‗C1'and bent Samples ‗C2'are 0.511% and 0.068% respectively. This represents a reduction of 0.443%, implying the variations in load application has affected the percentage strain of the specimen

5.2.2 Main Findings for mechanical Properties of Bent and Welded Mild Steel Pipes

i. The Ultimate Tensile Strength (UTS) of Specimen ‗L' and Specimen ‗C' of the welded L-Shaped specimen and the bent C -Shape Specimen are 77.273 MPa, and 62.216 MPa respectively, indicating a reduction of 15.057 MPa in the UTS of the sample L. This represents a drop 19.485% of the initial welded sample UTS value of 77.273MPa. This means that the welding process has resulted in making the L – shape sample more Brittle and harder and will required a higher load to fail and hence a higher UTS value of the L - shape sample. Also, the curve shape sample C, was ductile and soft which make the C – Shape sample to stretch more and hence lower UTS value.

ii. The load at Yield Point of Specimen ‗L' and Specimen ‗C' of the welded L-Shaped specimen and the bent C–shape specimen are 6.8KN, and 5.475KN respectively, indicating a reduction of 1.325KN in the load Yield Point of the L-shape sample. This represents a percentage drop 19.48% of the welded sample, an indication that, the process of welding has resulted in increasing the brittleness of the welded sample thereby increasing the yield load and Yield Strength of the Specimen L.

iii. The Elastic Moduli of Specimen ‗L' and Specimen ‗C' of the welded L-Shaped specimen and the bent C–shape specimen are 75GPa, and 49GPa respectively. This indicates a marginal reduction in the Elastic modulus of 26GPa and a percentage drop 53.06% of the welded sample, an indication that, the process of welding has given rise to the highest Elastic modulus of the welded sample.

iv. The percentage strain of Specimen ‗L' at a load of 6.8KN was 0. 511% and the percentage strain of Specimen ‗C' at a load of 5.475 was to 0.068%. This shows that a reduction in load applied adversely affects the percentage strain of about 19.48%.

5.2.3 Main Findings for Deformation and Fracture Characteristics of Bent and Welded Mild Steel Pipes

i. Main Findings on Tensile Test Results

The load applied to specimen ‗L' the welded Sample and specimen ‗C the bent Sample are 6.8KN and 5.475KN respectively. The load dropped to 1.325KN when bent without welding. This represents a percentage drop of 19.48% of the welding sample, an indication that the welding process induces more stress in the heat affected zone on the sample making it Brittle and harder which will causes the sample to permanently deform at a higher load. On the other hand, the bending process also makes sample ‗C' strain, Tougher and Ductile which make the sample to stretch at a maximum displacement far greater than the L- shape sample. This conforms to available literature by Sklenicka that a marginal increase in displacement as a result of an increase in loads and strain, will leads to an increase in deformation and vice versa.

ii. Main Findings on Impact analysis

(a) The equivalent (Von mises) stress of the ‗L' shape sample and ‗C' shape samples based on distortion energy failure theory. The tensile test simulation results shows that with the L-shape sample whose welded joint at the centre were held fixed and was subjected to a fixed

(b) The ‗L' shape sample displaces far from the extreme ends when a fixe load is applied to the sample. The red spots indicate the highest points of displacement and the yellow spots represents the medium spots of displacement, whiles the blue spots

represent least displace zone. However in the case of the bent shape sample, during the process of bending the part that was made to move to form the bent also becomes the most stress zone and most displace zone.

(c)   The most strain sample is the bent sample. This is because the process only resulted in making the curve zone strain, and the sample becomes more ductile than the welded sample. However, in the case of the l-shape sample, the welding process introduces more carbon into the sample making the sample brittle. This makes sample L requires a larger load to fail or deformed

iii. Main Findings on Microstructure analysis:

These results imply that the electric arc welding processes of specimen 'Negatively affected the Ultimate Tensile Strength, Yield Strength and Elastic Moduli of the material studied (i.e. low carbon steel). The results also suggest that low carbon steel specimen components (Specimen _C' bent specimens and unbent specimen _S') can withstand lower tensile stresses than when the components are welded.

The strain results suggest that the material studied became slightly more Brittle after welding. This can be attributed to the heat induced during the process of welding and bending the sample specimen.

The impact test results suggest that the bent pipe which has low carbon steel components can withstand low impact loads than the welded low carbon steel components. This is largely consistent with available literature, which states that the mechanical properties of a material are internal parameters that do not change substantially unless the properties are purposefully manipulated with external factors such as bending, welding, doping, heat and surface treatment among others. The ferrites (grey spots) distribution in the micrographs of the _L' shape welded samples increased remarkably. This can be seen in the near-even distribution of pearlite and

ferrite grains in the micrographs of the welded samples specimen. The increase in the grain size (quantity) of ferrites is attributed to the addition of ferrites from the welding electrode and bending into the microstructures of the samples, during the welding and bending process and the recrystallization of the grains.

The study did not establish a clear-cut relationship between the welded and bent samples, and their Ultimate Tensile and Yield Strengths of both the welded and bent samples.

However, the study established a negative (inverse) relationship between the welded and the bent samples.

5.3 Conclusion

From the results obtained and the analyses done, it can be stated that the welding processes adversely affected the Ultimate Tensile Strength (UTS), Yield Strength, Elastic Modulus and Impact Strength of the samples studied; since all the samples studied had their Ultimate Tensile Strength, Yield Strength, Elastic Moduli and Impact dropped after undergoing welding and bending. However, the strain of the samples increased after subjecting the samples to welding, bending and testing. The increase in strain of the welded samples is attributable to the heat induced during the electric arc welding processes. The grain structure of the samples studied, improved after welding; as there is a near even distribution of pearlites (dark spots) and ferrites (gray spots) in the micrographs of samples after welding and bending. The improvement in the grain size (structure) is attributable to the introduction of additional grains from the welding electrode during the processes of welding and recrystallization of the grains as a result of heat treatment. This is largely consistent with available literature, which states that the mechanical properties of a material and

its internal parameters do not change substantially unless the properties are purposefully manipulated with external factors such as bending, welding, doping, heat and surface treatment among others. Also, the study did not establish a clear-cut relationship between the samples, and their Ultimate Tensile and Yield Strengths of both welded and bent samples. This is largely consistent with available literature which states that the Ultimate Tensile Strength and Yield Strength are internal properties of a material, which do not change substantially. Any significant changes in these properties can be attributable to heat treatment, welding and bending processes. However, the study established a negative (inverse) relationship between the Strain percentage. The strain of the welded and bent samples reduced consistently. This means that bent and welded samples can withstand higher tensile loads or forces than the straight samples.

5.4 Recommendations

It is recommended that future studies on mechanical strength of engineering materials (especially metals pipes) should include a comparative analysis bent and bent welded pipes to obtain a comprehensive understanding of the mechanical properties of the pipes; as this study has shown that there is a relationship between bent and welded pipes and some mechanical properties of the material studied. Using a single diameter to conduct studies on the mechanical properties of materials may lead to inaccurate results and conclusion. Also, welding and bending of low Carbon Steel components and for that matter, any other metal components should be standardized and regulated as this study has established that some important mechanical properties of the samples studied, were adversely affected by the process of bending and welding. The process of standardization and regulation of the welding profession and bending of pipes can

be achieved through training and certification of professionals and metal artisans. It is further recommended that, just like AISI and ASTM of North America, a regulatory and standardization body be set up to help streamline and properly regulate the metal fabrication industry in the country, the sub region and the continent of Africa as a whole.

5. 5 Suggestions for Further Research

It is suggested that further research be carried out on other important industrial materials since this study was limited to only mild steel. It is also suggested that other methods of welding and bending be applied on the sample pipes studied to determine the most suitable method of welding and bending square metals pipes. Again, where applicable and appropriate, other pepe welding and bending methods such as riveting, bolting, soldering, brazing among others, should be used to join or bend pipes in order to avoid the negative effects of welding and bending of pipes. Furthermore, heat-treatment should be carried out on welded and bend pipes systems after welding and bending them. This is necessary to relieve or reduce the effects of residual and thermal stresses at the Heat Affected Zone (HAZ) during the process of welding and bending. Cost analyses of welding and bending metals pipes should be conducted to ascertain the most cost-effective method of welding and bending industrial metals pipes.

REFERENCES

Abdulhameed, D., Martens, M., Cheng, J. R., & Adeeb, S. (2017, July). Investigation of Smooth Pipe Bends Under the Effect of In-Plane Bending. In *Pressure Vessels and Piping Conference* (Vol. 57946, p. V03AT03A054). American Society of Mechanical Engineers.

ASME B31.1: Power piping. ASME Code for pressure piping.

ASME B31.3 and CSA Z662-15.

ASME B31.3: Process piping code. ASME Code for pressure piping.

ASTM A370. (2014). Standard Test Methods and Definitions for Mechanical Testing of Steel Products. In Annual Book of ASTM Standards. West Conshohocken, PA: ASTM International. Retrieved from   www.astm.org

ASTM A881/A881M. (2015). Standard Specification for Steel Wire, Indented, Low-Relaxation for Prestressed Concrete Railroad Ties. In Annual Book   of ASTM Standards. West Conshohocken, PA: ASTM   International. Retrieved from www.astm.org

ASTM E8/E8M. (2015). Standard Test Methods for Tension Testing of Metallic Materials. In Annual Book of ASTM Standards. West Conshohocken, PA: ASTM International.

ASTM International. (2004). Tensile Testing - Chapter 1 : Introduction to Tensile Testing. (Second). Materuals Park, OH, USA. Retrieved 09 2015, from http://www.asminternational.org/documents/10192/3465262/05105G_Chapter _1.pdf/e13 396e8-a327-490a-a414-9bd1d2bc2bb8

ASTM International. (2004). Tensile Testing - Chapter 1 : Introduction to Tensile Testing. (Second). Materuals Park, OH, USA. Retrieved 09 2015, from

http://www.asminternational.org/documents/10192/3465262/05105G_Chapter _1.pdf/e13 396e8-a327-490a-a414-9bd1d2bc2bb8

Beer, F. P., Johnston, E. R., DeWolf, J. T., & Mazurek, D. F. (2015). Mechanics of Materials. (Seventh, Ed.) New York: Mc Graw Hill Education.

Byars, E. F., Snyder, R. D., & Plants, H. L. (1925). Engineering Mechanics of Deformable 67 Bodies. New York: Harper & Row.

Byars, E. F., Snyder, R. D., & Plants, H. L. (1983). *Engineering mechanics of deformable bodies*. HarperCollins College Division

Callister, D. W., & Rethwisch, D. G. (2007). Magnetic properties. *Materials Science and Engineering, An Introduction, 7th Ed. ed. John Willey & Sons, Inc*, 19-56.

Callister, W. D. (2001). Fundamentals of Materials Science and Engineering John Wiley & Sons. *Inc, New York*.

Chen, Y. S. (2016). *Testing and modeling tensile stress-strain curve for prestressing wires in railroad ties* (Doctoral dissertation, Kansas State University).

Clark, R. A., & Reissner, E. (1951). Bending of curved tubes. *Advances in applied mechanics*, *2*, 93-122.

Deshmukh, S. P., Rao, A. C., Gaval, V. R., & Mahanwar, P. A. (2011). Mica-filled PVC composites: effect of particle size, filler concentration, and surface treatment of the filler, on mechanical and electrical properties of the composites. *Journal of Thermoplastic Composite Materials*, *24*(5), 583-599.

Gedney, R. (2002). Guide to Testing. *Advanced materials & processes*, 29.

He, Y., Heng, L., Zhang, Z., Mei, Z. H. A. N., Jing, L. I. U., & Guangjun, L. (2012). Advances and trends on tube bending forming technologies. *Chinese Journal of Aeronautics*, *25*(1), 1-12.

He, Y., Heng, L., Zhang, Z., Mei, Z. H. A. N., Jing, L. I. U., & Guangjun, L. (2012). Advances and trends on tube bending forming technologies. *Chinese Journal of Aeronautics*, *25*(1), 1-1

Heidarpour, A., Tofts, N. S., Korayem, A. H., Zhao, X. L., & Hutchinson, C. R. (2014). Mechanical properties of very high strength steel at elevated temperatures. *Fire safety journal*, *64*, 27-35.

Hosford, W. F. (1992). Overview of tensile testing. *ASM International, Tensile Testing(USA), 1992,*, 1-24.

Hosseini, S., Heidarpour, A., Collins, F., & Hutchinson, C. R. (2016). Strain ageing effect on the temperature dependent mechanical properties of partially damaged structural mild-steel induced by high strain rate loading. *Construction and Building Materials*, *123*, 454-463.

http://www.onlinemetals.com/alloycat.cfm?alloy=1018

http://www.onlinemetals.com/alloycat.cfm?alloy=A36

Khayal, O. M. E. S. (2019). Laboratory Experiments Tensile Testing. *Res. Gate*.

Lubis, A., & Boyle, J. T. (2004). The pressure reduction effect in smooth piping elbows—revisited. *International journal of pressure vessels and piping*, *81*(2), 119-125.

Malek, A. Z. A. (2012). *Experimental and Simulation Study on the Effect of Friction in a Four-Point Bending Test (4PB)* (Doctoral dissertation, UMP).

Rodabaugh, E., & George, H. H. (1957). Effect of internal pressure on flexibility and stress-intensification factors of curved pipe or welding elbows. *Transactions of the American Society of Mechanical Engineers*, *79*(4), 939-948.

Sellakumar, S., & Venkatasamy, R. (2013). Review of structural assessment of pipe bends. *International review of mechanical engineering*, 1180-88.

Shakya, A. M., & Kodur, V. K. R. (2016). Effect of temperature on the mechanical properties of low relaxation seven-wire prestressing strand. *Construction and Building Materials*, *124*, 74-84.

Sklenička, V., Kuchařová, K., Král, P., Kvapilová, M., Svobodová, M., & Čmakal, J. (2015). The effect of hot bending and thermal ageing on creep and microstructure evolution in thick-walled P92 steel pipe. *Materials Science and Engineering: A*, *644*, 297-309.

von Karman, T. (1911). On the deformation of thin-walled pipes especially of elastic expansion pipes. *Z. Ver. dtsch. Ing*, *55*, 1889.

Wen, T. (2014). On a new concept of rotary draw bend-die adaptable for bending tubes with multiple outer diameters under non-mandrel condition. *Journal of Materials Processing Technology*, *214*(2), 311-317.

Whitney, C. S. (1937, March). Design of reinforced concrete members under flexure or combined flexure and direct compression. In *Journal Proceedings* (Vol. 33, No. 3, pp. 483-498)

William F.. Smith, & Hashemi, J. (2006). *Foundations of materials science and engineering*. Mcgraw-Hill Publishing.

Zong, Z., Jiang, D., & Zhang, J. (2015). Study of the mechanical performance of Grade 1860 steel wires at elevated temperatures. *Materials Research Innovations*, *19*(sup5), S5-1175.

APPENDICES

APPENDIX A

Appendix A. Nomenclature

AISI - American Iron and Steel Institute

L - Welded sample specimen

C – Bent sample specimen

S – Straight sample specimen

ASME - American Society of Mechanical Engineers

NPS - Nominal pipe size

R - Bend radius

α - Bend angles

CAD - computer-aided design

CAE - computer-aided engineering

FEM - finite element modeling

high-strength CDS AISI 1018

steel strength than HSS and VHS steel grades with martensite microstructures

ASTM - The American Society for Testing and Materials

Do – diameter of the specimen

Ao - cross-sectional area of the specimen

Py - load at yielding

σy - yield stress

Ao- original cross-sectional area of the specimen

σ w - allowable working strength

σ TS (UTS) - the ultimate tensile strength,

EUL - extension-under-load method

σu - Ultimate strength

E - Young's modulus

UR - modulus of resilience

SEM

σ - engineering stress

ε - engineering strain

P - external axial tensile load

Lo - original length of the specimen
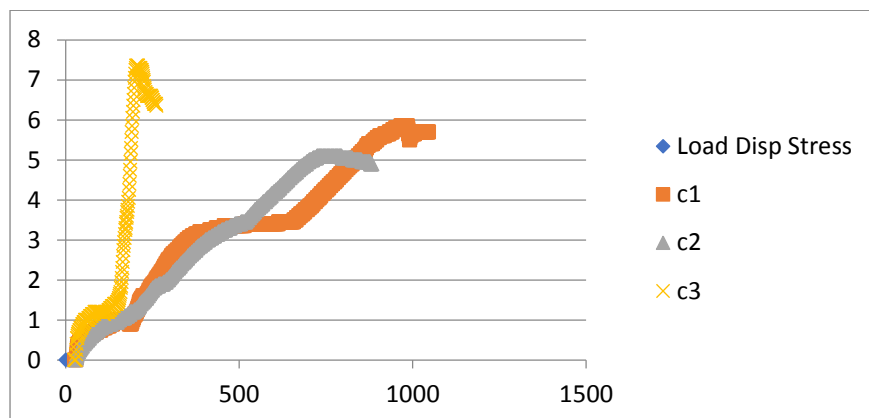
Lf - final length of the specimen

SE(B) - single-edge bend

HAZ - heat affected zone

APPENDIX B. Load Displacement Graphs

Appendix B. 1 Load displacement graph for C – shape Sample

Appendix B. 2 Load displacement graph for L – shape Sample
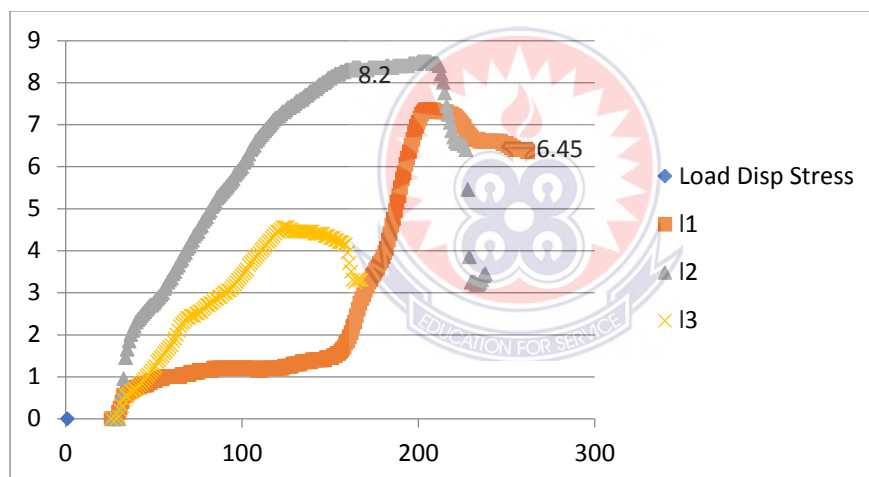
Appendix B. 3 Load displacement graph for S – shape Sample

71
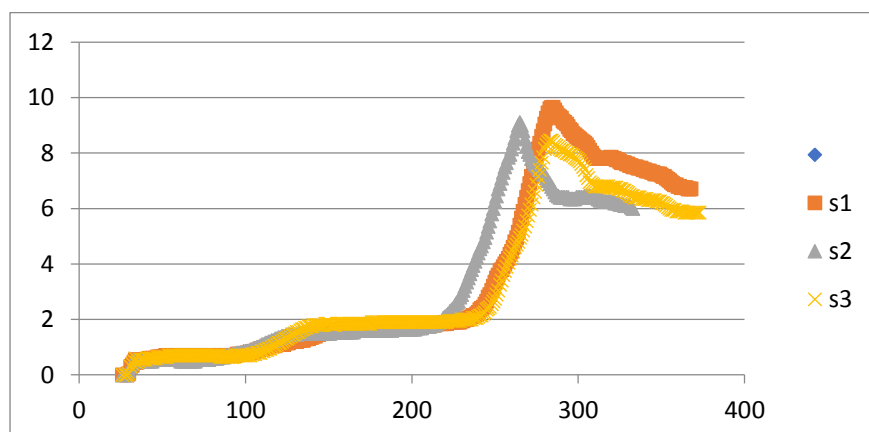
APPENDIX C Simulation Results for L – Shape Specimen

Appendix C. 1 Mesh Model for L – shape Sample
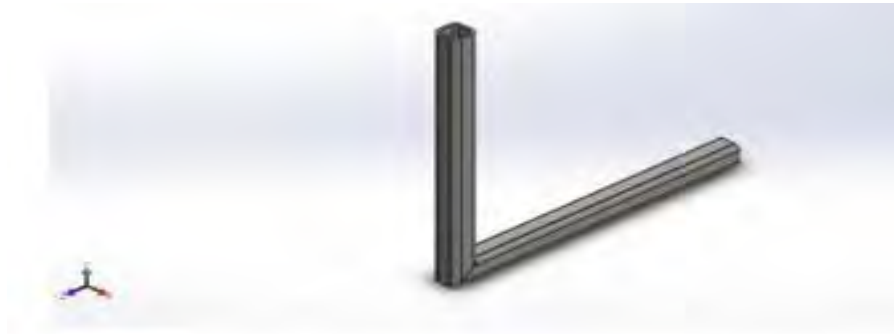
Appendix C. 2 Impact test for L – shape Sample

Model name: L-TYPE SQUARE TUBE. impact test
Current Configuration: Default
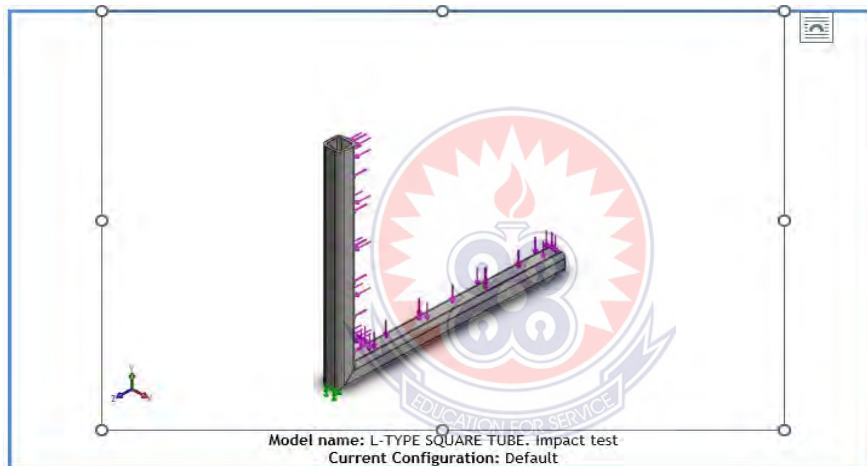
Appendix C. 3 Volumetric Properties for L – shape Sample

Solid Bodies			
Document Name and Reference	Treated As	Volumetric Properties	Document Path/Date Modified
L-TYPE SQUARE TUBE.stp	Solid Body	Mass:0.556111 kg Volume:7.03938e-05 m^3 Density:7,900 kg/m^3 Weight:5.44989 N	C:\Program Files\SOLIDWORKS Corp\SOLIDWORKS\NF EN 10219-2 - 25 x 25 x 3 - 304.8.stp.SLDPRT

| L-TYPE SQUARE TUBE.stp | Solid Body | Mass:0.556111 kg Volume:7.03938e-05 m^3 Density:7,900 kg/m^3 Weight:5.44989 N | C:\Program Files\SOLIDWORKS Corp\SOLIDWORKS\NF EN 10219-2 - 25 x 25 x 3 - 304.8_1.stp.SLDPRT |
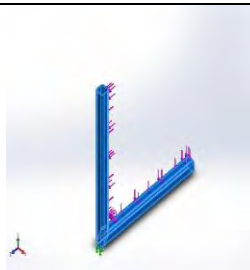
Appendix C. 4 Study Properties for L – shape Sample

Study name	Static 3
Analysis type	Static
Mesh type	Solid Mesh
Thermal Effect:	On
Thermal option	Include temperature loads
Zero strain temperature	298 Kelvin
Include fluid pressure effects from SOLIDWORKS Flow Simulation	Off
Solver type	FFEPlus
Inplane Effect:	Off
Soft Spring:	Off
Inertial Relief:	Off
Incompatible bonding options	Automatic
Large displacement	On
Compute free body forces	On
Friction	Off
Use Adaptive Method:	Off
Result folder	SOLIDWORKS document (C:\Users\HP)
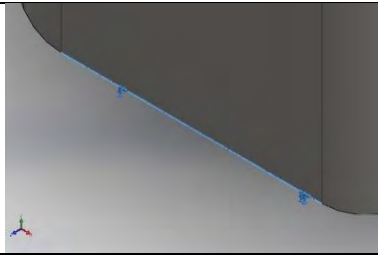
Appendix C. 5 Units for L – shape Sample

Unit system:	SI (MKS)
Length/Displacement	Mm
Temperature	Kelvin
Angular velocity	Rad/sec
Pressure/Stress	N/m^2
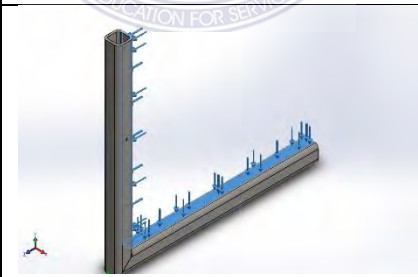
Appendix C. 6 Material Properties for L – shape Sample

Model Reference	Properties		Components
	Name:	AISI 1018	SolidBody 1(L-TYPE SQUARE TUBE.stp)(Frame0 001.stp-1/NF EN 10219-2 - 25 x 25 x 3 - 304.8.stp-1), SolidBody 1(L-TYPE SQUARE TUBE.stp)(Frame0 001.stp-1/NF EN 10219-2 - 25 x 25 x 3 - 304.8_1.stp-1)
	Model type:	Linear Elastic Isotropic	
	Default failure criterion:	Max von Mises Stress	
	Yield strength:	3.51571e+08 N/m^2	
	Tensile strength:	4.20507e+08 N/m^2	
	Elastic modulus:	2e+11 N/m^2	
	Poisson's ratio:	0.29	
	Mass density:	7,900 kg/m^3	
	Shear modulus:	7.7e+10 N/m^2	
	Thermal expansion coefficient:	1.5e-05 /Kelvin	
Curve Data:N/A			
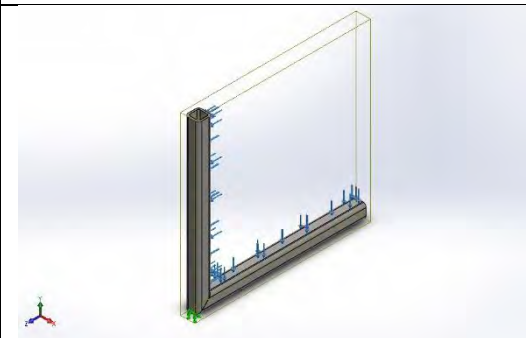
Appendix C. 7 Loads and Fixture for L – shape Sample

Fixture name	Fixture Image	Fixture Details	
Fixed-1		Entities:	1 edge(s)
		Type:	Fixed
			Geometry
Resultant Forces			
Components	X	Y	Z	Resultant
Reaction force(N)	-293.4	63,816	-56,957.2	85,537.7
Reaction Moment(N.m)	0	0	0	0

Appendix C. 8 Loads Image for L – shape Sample

Load name	Load Image	Load Details	
Force-1		Entities:	2 face(s)
		Type:	Apply
			normal
			force
		Value:	15,000
			kgf

Appendix C. 9 Contact Information for L – shape Sample

Contact	Contact Image	Contact Properties
Global Contact		Type: Bonded Components: 1component(s) Options: Incompatible mesh

Appendix C. 10 Mesh Information for L – shape Sample

Mesh type	Solid Mesh
Mesher Used:	Standard mesh
Automatic Transition:	Off
Include Mesh Auto Loops:	Off
Jacobian points for High quality mesh	16 Points
Element Size	5.70271 mm
Tolerance	0.285135 mm
Mesh Quality	High
Remesh failed parts with incompatible mesh	Off

Appendix C. 11 Mesh information- Details for L – shape Sample

Total Nodes	17867
Total Elements	8841
Maximum Aspect Ratio	6.6019
% of elements with Aspect Ratio < 3	98.6

% of elements with Aspect Ratio < 10	0
% of distorted elements(Jacobian)	0
Time to complete mesh(hh: mm;ss):	00:00:03
Computer name:	

Appendix C. 12 Mesh model for L – shape Sample
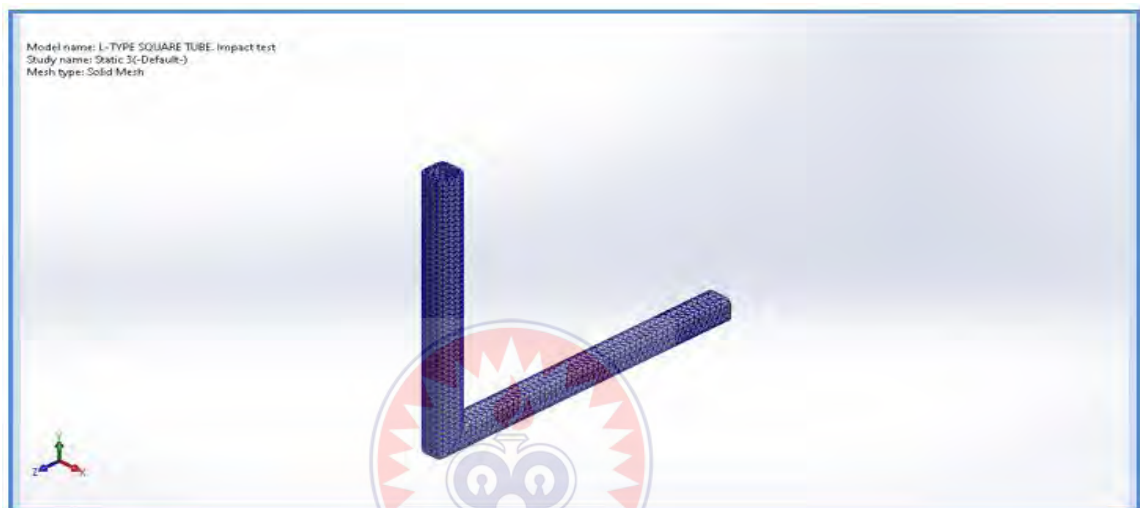
Appendix C. 13 Resultant Forces or L – shape Sample

Selection set	Units	Sum X	Sum Y	Sum Z	Resultant
Entire Model	N	-255.156	43,811.4	-158,649	164,587

Appendix C. 14 Reaction Moments for L – shape Sample

Selection set	Units	Sum X	Sum Y	Sum Z	Resultant
Entire Model	N.m	0	0	0	0

Appendix C. 15 Free body Forces for L – shape Sample

Selection set	Units	Sum X	Sum Y	Sum Z	Resultant
Entire Model	N	0	0	0	0

Appendix C. 16 Free body moments for L – shape Sample

Selection set	Units	Sum X	Sum Y	Sum Z	Resultant
Entire Model	N.m	0	0	0	0

Appendix C. 17 Study results for L – shape Sample

Name	Type	Min	Max
Stress1	VON: von Mises Stress	8.102e+06N/m^2 Node: 2935	1.596e+10N/m^2 Node: 17679

L-TYPE SQUARE TUBE. Impact test-Static 3-Stress-Stress1
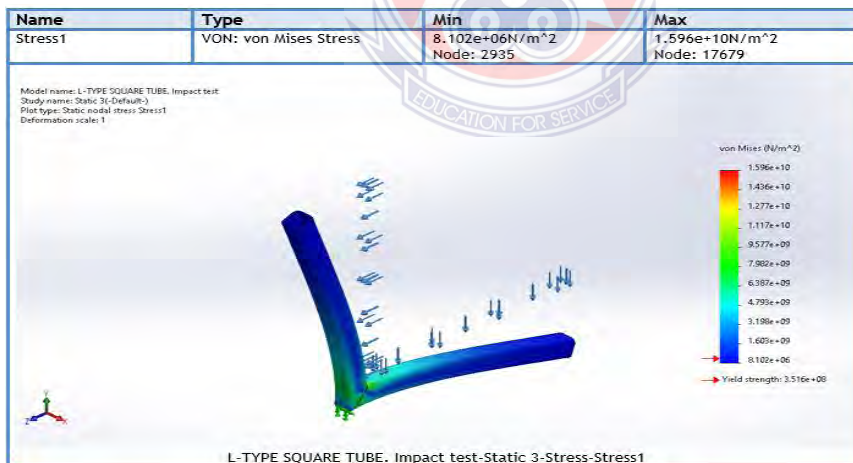
Appendix C. 18 Resultant Displacement for L – shape Sample

Name	Type	Min	Max
Displacement1	URES: Resultant Displacement	0.000e+00mm Node: 8955	7.292e+01mm Node: 9650

L-TYPE SQUARE TUBE. Impact test-Static 3-Displacement-Displacement1

Appendix C. 19 Equivalent Strain for L – shape Sample

Name	Type	Min	Max
Strain1	ESTRN: Equivalent Strain	5.700e-05 Element: 6618	4.802e-02 Element: 6588

Appendix C. 20 Deformed shape for L – shape Sample

Name	Type
Displacement1{1}	Deformed shape

L-TYPE SQUARE TUBE. Impact test-Static 3-Displacement-Displacement1{1}

79
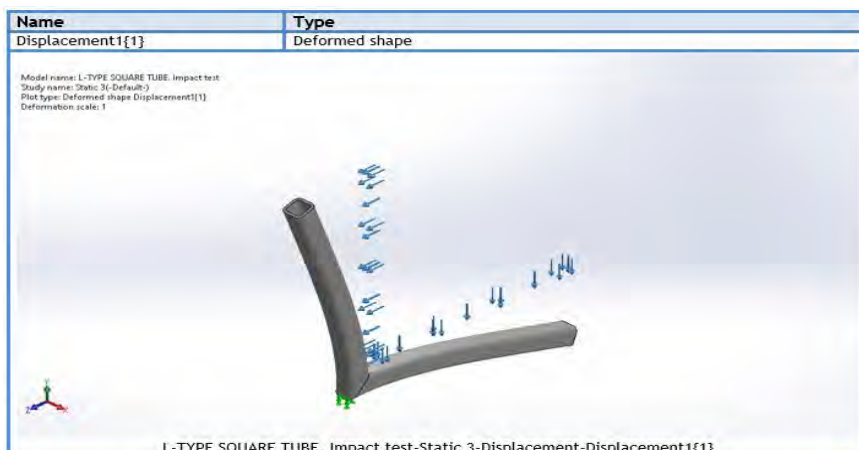
Appendix C. 21 Graph for Deformed for L – shape Sample
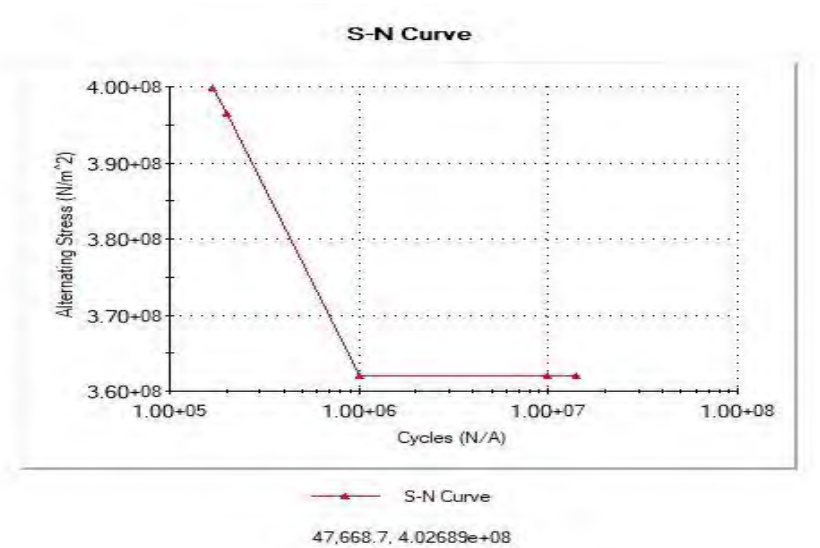
APPENDIX D SIMULATION OF IMPACT TEST ON BENT SQUARE TUBE

Appendix D. 1 Mesh for C – shape Sample

Appendix D. 2 Model Information for C – shape Sample

Model name: BENT SQUARE TUBE .impact test
Current Configuration: Default

80

Appendix D. 3 Volumetric Properties for C – shape Sample

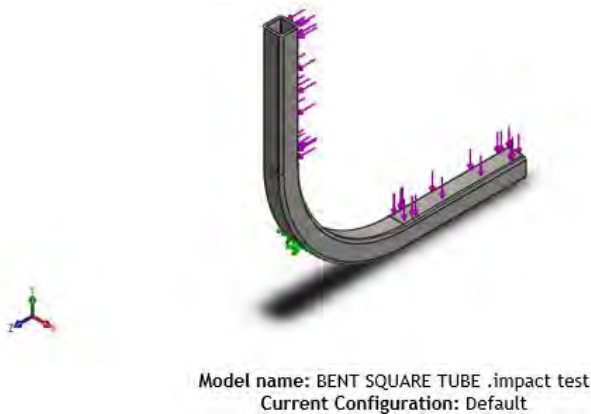| Solid Bodies			
Document Name and Reference	Treated As	Volumetric Properties	Document Path/Date Modiefied
BENT SQUARE TUBE .stp	Solid Body	Mass:1.12041 kg Volume:0.000141824 m^3 Density:7,900 kg/m^3 Weight:10.98 N	C:\Program Files\SOLIDWORKS Corp\SOLIDWORKS\ASTM A513 - 1 x 1 x 3_25 - 21.465.stp.SLDPRT

Appendix D. 4 Study Properties for C – shape Sample

Study	Static 1
Analysis type	Static
Mesh type	Solid Mesh
Thermal Effect:	On
Thermal option	Include temperature loads
Zero strain temperature	298 kelvin
Include fluid pressure effects from SOLIDWORKS Flow Simulation	Off
Solver type	FFEPlus
Inplane Effect	Off
Soft Spring:	Off

Inertial Relief	Off
Incompatible bonding options	Automatic
Large displacement	On
Compute free body forces	On
Friction	Off
Use Adaptive Method:	Off
Result folder	

Appendix D. 5 Units for C – shape Sample

Unit system:	SI (MKS)
Length/Displacement	**Mm**
Temperature	Kelvin
Angular velocity	Rad/sec
Pressure/Stress	N/m^2

Appendix D. 6 Material Properties for C – shape Sample

Model Reference	Properties		Components
	Name:	AISI 1018	SolidBody
	Model type:	Linear Elastic	1(BENT SQUARE
		Isotropic	TUBE
	Default failure	Max von Mises	.stp)(Frame0001.st
	criterion:	Stress	p-1/ASTM A513 -
	Yield strength:	3.51571e+08	1 x 1 x 3_25 -
		N/m^2	21.465.stp-1)
	Tensile strength:	4.20507e+08	
		N/m^2	
	Elastic modulus:	2e+11 N/m^2	
	Poisson's ratio:	0.29	
	Mass density:	7,900 kg/m^3	
	Shear modulus:	7.7e+10 N/m^2	
	Thermal expansion	1.5e-05 /Kelvin	
	coefficient:		
Curve Data: N/A			

Appendix D. 7 Load and Fixtures for C – shape Sample

Fixture name	Fixture Image	Fixture Detail	
Fixed-1		Entities:	1 edge(s)
		Type:	Fixed
			Geometry
Resultant Forces			
Components	X	Y	Z	Resultant
Reaction force(N)	-0.00549316	7,354.99	-7,354.99	10,401.5
Reaction Moment (N.m)	0	0	0	0

Appendix D. 8 Load image for C – shape Sample

Load name	Load Image	Load Details	
Force-1		Entities:	2 face(s)
		Type:	Apply
			normal
			force
		Value:	15,000
			kgf

Appendix D. 9 Mesh information for C – shape Sample

| Mesh type	Solid Mesh
Mesher Used:	Standard mesh
Automatic Transition	Off
Include Mesh Auto Loops:	Off

Jacobian points for High quality mesh	16 Points
Element Size	5.35859 mm
Tolerance	0.267929 mm
Mesh Quality	High
Remesh failed parts with incompatible mesh	Off

Appendix D. 10 Mesh information – Details for C – shape Sample

Total Nodes	21186
Total Elements	10735
Maximum Aspect Ratio	24.671
% of elements with Aspect Ratio < 3	81.8
% of elements with Aspect Ratio < 10	6.64
% of distorted elements(Jacobian)	0
Time to complete mesh (hh: mm: ss)	00:00:04
Computer name:	

Appendix D. 11 Mesh model for C – shape Sample
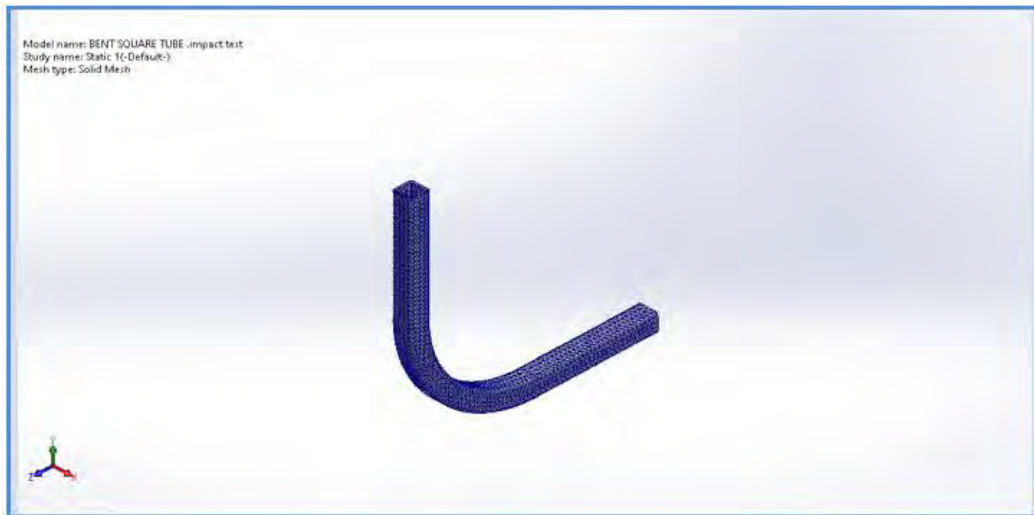
Appendix D. 12 Resultant Forces for C – shape Sample

Selection set	Units	Sum X	Sum Y	Sum Z	Resultant
Entire Model	N	-0.00549316	7,354.99	-7,354.99	10,401.5

Appendix D. 13 Reaction Moments for C – shape Sample

Selection set	Units	Sum X	Sum Y	Sum Z	Resultant
Entire Model	N.m	0	0	0	0

Appendix D. 14 Free body Forces for C – shape Sample

Selection set	Units	Sum X	Sum Y	Sum Z	Resultant
Entire Model	N	0	0	0	0

Appendix D. 15 Free body moments for C – shape Sample

Selection set	Units	Sum X	Sum Y	Sum Z	Resultant
Entire Model	N.m	0	0	0	0

Appendix D. 16 von Mises Stress for C – shape Sample
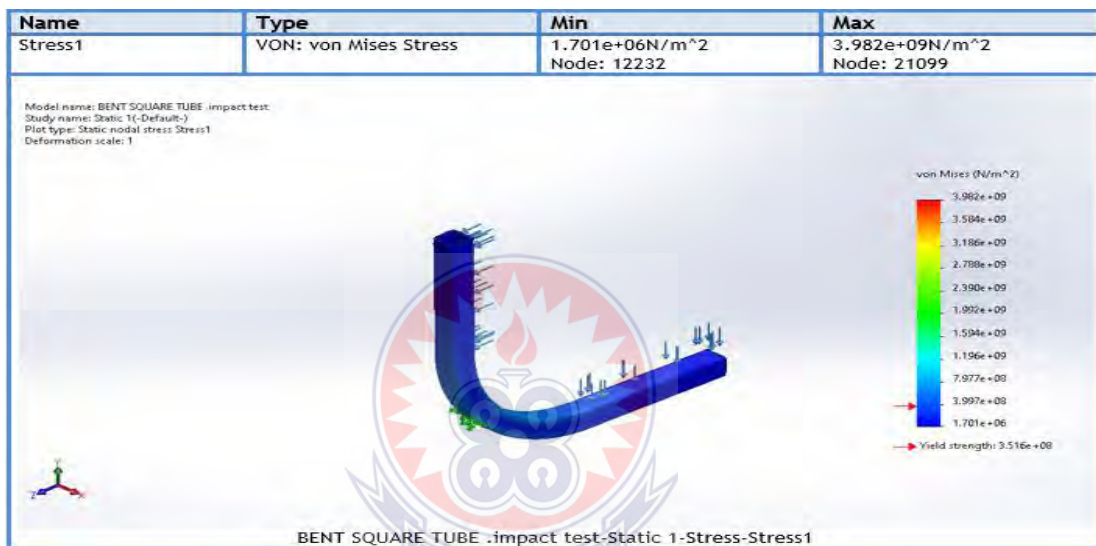
Appendix D. 17 Resultant displacement for C – shape Sample
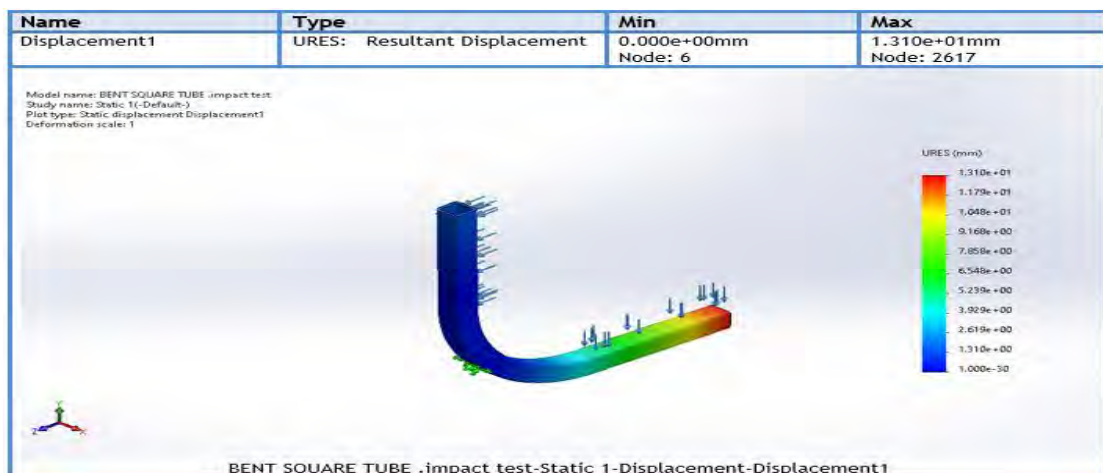
Appendix D. 18 Equivalent Strain for C – shape Sample

Name	Type	Min	Max
Strain1	ESTRN: Equivalent Strain	3.950e-06 Element: 9081	8.967e-03 Element: 7178
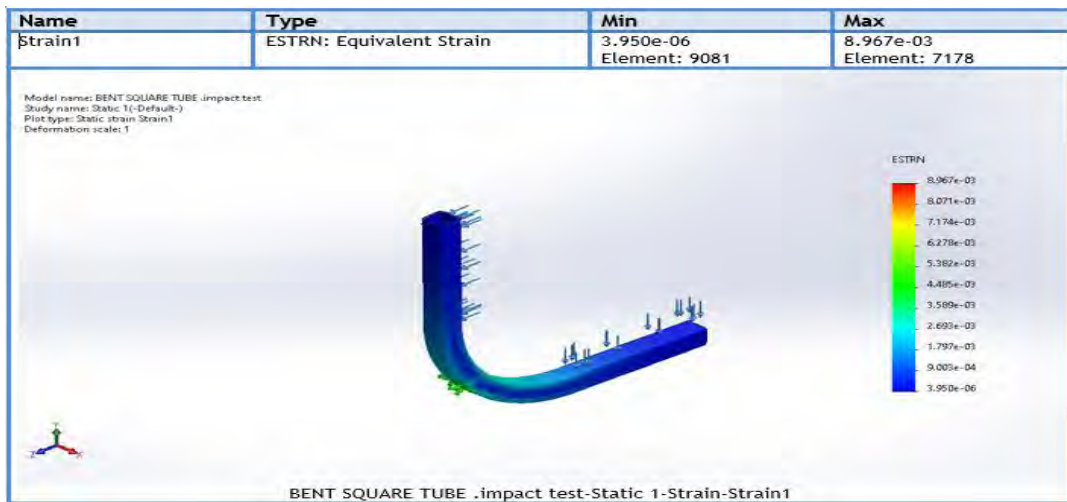
Appendix D. 19 Equation for von Mises stress for C – shape Sample

Name	Type	Min	Max
Equation1	"VON: von Mises Stress"	1.701e+06SI Node: 12232	3.982e+09SI Node: 21099
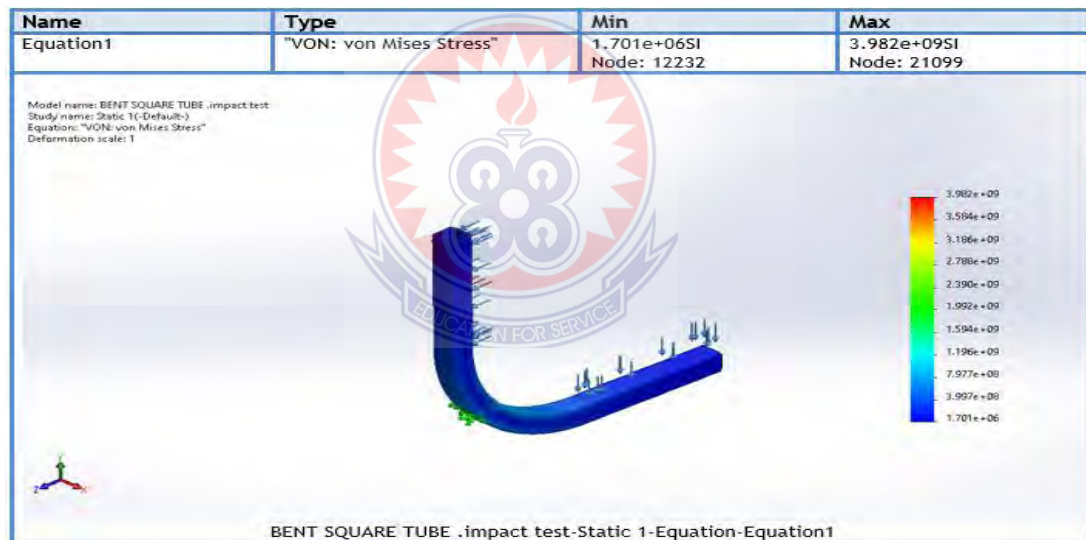
Appendix D. 20 Factor of safety for C – shape Sample

Name	Type	Min	Max
Factor of Safety1	Automatic	8.830e-02 Node: 21099	3.000e+00 Node: 33

BENT SQUARE TUBE .impact test-Static 1-Factor of Safety-Factor of Safety1
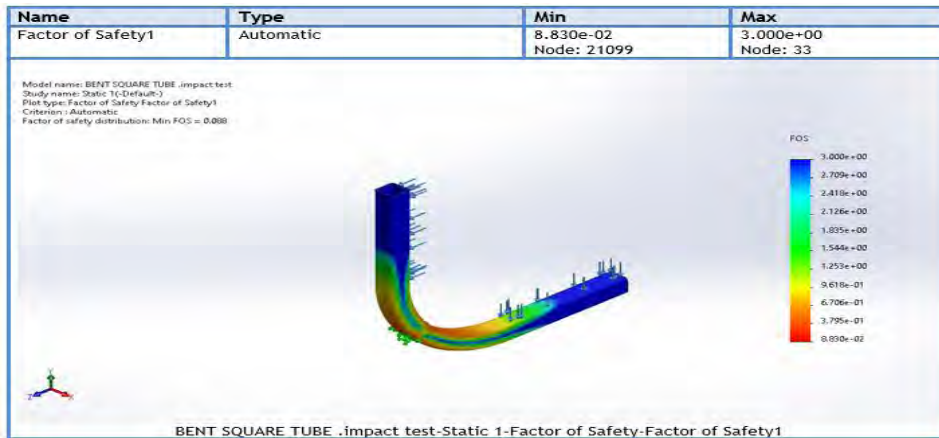
Appendix D. 21 Stress Graph for deformed C – shape Sample

Image-1

APPENDIX E SIMULATION OF IMPACT TEST ON STRAIGHT TUBE
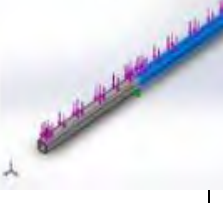
Appendix E. 1 Impact test model for S – shape Sample
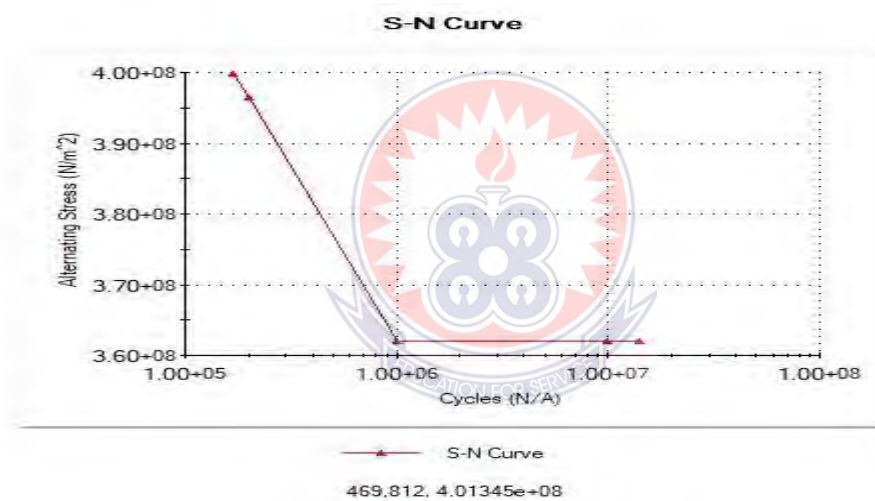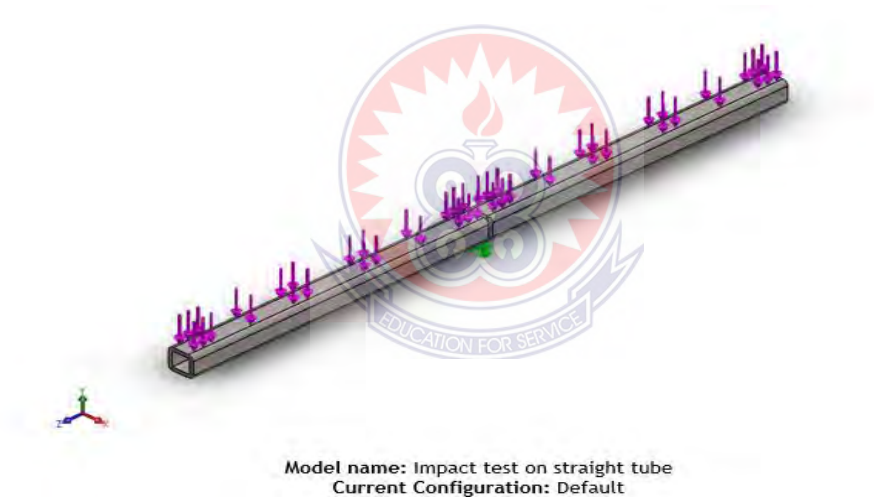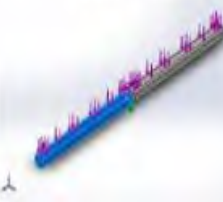

Appendix E. 2 Model Information for S – shape Sample

Model name: Impact test on straight tube
Current Configuration: Default

Appendix E. 3 Volumetric Properties for S – shape Sample

Solid Bodies			
Document Name and Reference	**Treated As**	**Volumetric Properties**	**Document Path/Date Modified**
Chamfer1	Solid Body	Mass:0.759224 kg Volume:9.61043e -05 m^3 Density:7,900 kg/m^3 Weight:7.44039 N	C:\Users\HP\Documents\soldworks \shraight shap specimen (S2)joint.SLDPRT Sep 8 15:31:34 2021
Chamfer1	Solid Body	Mass:0.759224 kg Volume:9.61043e -05 m^3 Density:7,900 kg/m^3 Weight:7.44039 N	C:\Users\HP\Documents\soldworks \shraight shap specimen (S2)joint.SLDPRT Sep 8 15:31:34 2021

91
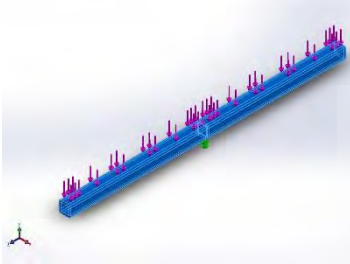
Appendix E. 4 Study Properties for S – shape Sample

Study	Static 1
Analysis type	Static
Mesh type	Solid Mesh
Thermal Effect:	On
Thermal option	Include temperature loads
Zero strain temperature	298 kelvin
Include fluid pressure effects from SOLIDWORKS Flow Simulation	Off
Solver type	FFEPlus
Inplane Effect	Off
Soft Spring:	Off
Inertial Relief:	Off
Incompatible bonding options	Automatic
Large displacement	On
Compute free body forces	
Friction	
Use Adaptive Method:	
Result folder	SOLIDWORKS document (C:\Users\HP\Documents\soldworks)
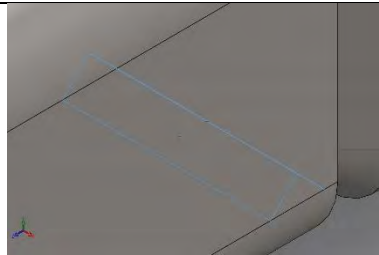
Appendix E. 5 for S – shape Sample

Units system	SI (MKS)
Length/Displacement	Mm
Temperature	Kelvin
Angular velocity	Rad/sec
Pressure/Stress	N/m²
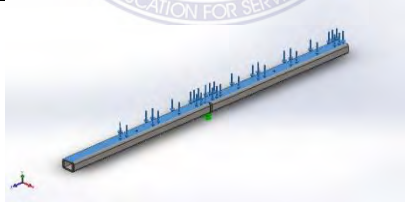
Appendix E. 6 Material Properties for S – shape Sample

Model Reference	Properties		Components
	Name:	AISI 1020	SolidBody
	Model type:	Linear Elastic	1(Chamfer1)(shr
		Isotropic	aight shap
	Default failure	Max von Mises	specimen
	criterion:	Stress	(S2)joint-1),
	Yield strength:	3.51571e+08 N/m^2	SolidBody
	Tensile strength:	4.20507e+08 N/m^2	1(Chamfer1)(shr
	Elastic modulus:	2e+11 N/m^2	aight shap
	Poisson's ratio:	0.29	specimen
	Mass density:	7,900 kg/m^3	(S2)joint-2)
	Shear modulus:	7.7e+10 N/m^2	
	Thermal expansion coefficient:	1.5e-05 /Kelvin	
Curve Data:N/A			
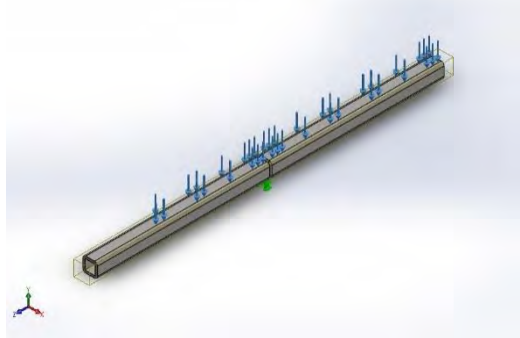
Appendix E. 7 Load and Fixtures for S – shape Sample

Fixture name	Fixture Image	Fixture Details	
Fixed-1		Entities:	**2 face(s)**
		Type:	**Fixed Geometry**
Resultant Forces			
Components	X	Y	Z	Resultant

Components	X	Y	Z	Resultant
Reaction force(N)	0.0898438	147,091	0.65918	147,091
Reaction Moment(N.m)	0	0	0	0

Appendix E. 8 Load image for S – shape Sample

Load name	Load Image	Load Details	
Force-1		Entities:	2 face(s)
		Type:	Apply normal force
		Value:	15,000 kgf

94

Appendix E. 9 Contact Information for S – shape Sample

Contact	Contact Image	Contact Properties	
Global Contact		Type:	Bonded
		Components:	1 component(s)
		Options:	Incompatible mesh

Appendix E. 10 Mesh information for S – shape Sample

Mesh type	Solid Mesh
Mesher Used:	Standard mesh
Automatic Transition:	Off
Include Mesh Auto Loops:	Off
Jacobian points for High quality mesh	16 Points
Element Size	6.28092 mm
Tolerance	0.314046 mm
Mesh Quality	High
Remesh failed parts with incompatible mesh	Off

Appendix E. 11 Mesh information - Details for S – shape Sample

Total Nodes	14526
Total Elements	7204
Maximum Aspect Ratio	5.1682
% of elements with Aspect Ratio < 3	87.7
% of elements with Aspect Ratio > 10	0
% of distorted elements(Jacobian)	0
Time to complete mesh(hh;mm;ss):	00:00:02
Computer name:	

Appendix E. 12 Mesh model for S – shape Sample
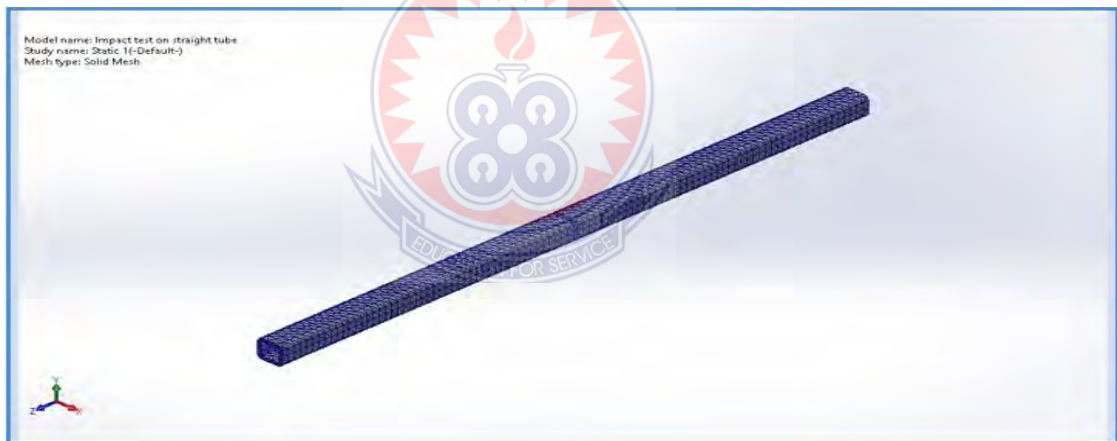
Appendix E. 13 Resultant Forces for S – shape Sample

Selection set	Units	Sum X	Sum Y	Sum Z	Resultant
Entire Model	N	403.368	145,921	145,786	206,268

Appendix E. 14 Reaction Moments S – shape Sample

Selection set	Units	Sum X	Sum Y	Sum Z	Resultant
Entire Model	N.m	0	0	0	0

Appendix E. 15 Free body Forces S – shape Sample

Selection set	Units	Sum X	Sum Y	Sum Z	Resultant
Entire Model	N	0	0	0	0

Appendix E. 16 Free body moments S – shape Sample

Selection set	Units	Sum X	Sum Y	Sum Z	Resultant
Entire Model	N.m	0	0	0	0

Appendix E. 17 Study Results S – shape Sample

Name	Type	Min	Max
Stress1	VON: von Mises Stress	4.916e+06N/m^2 Node: 7231	1.356e+10N/m^2 Node: 7085

Impact test on straight tube-Static 1-Stress-Stress1
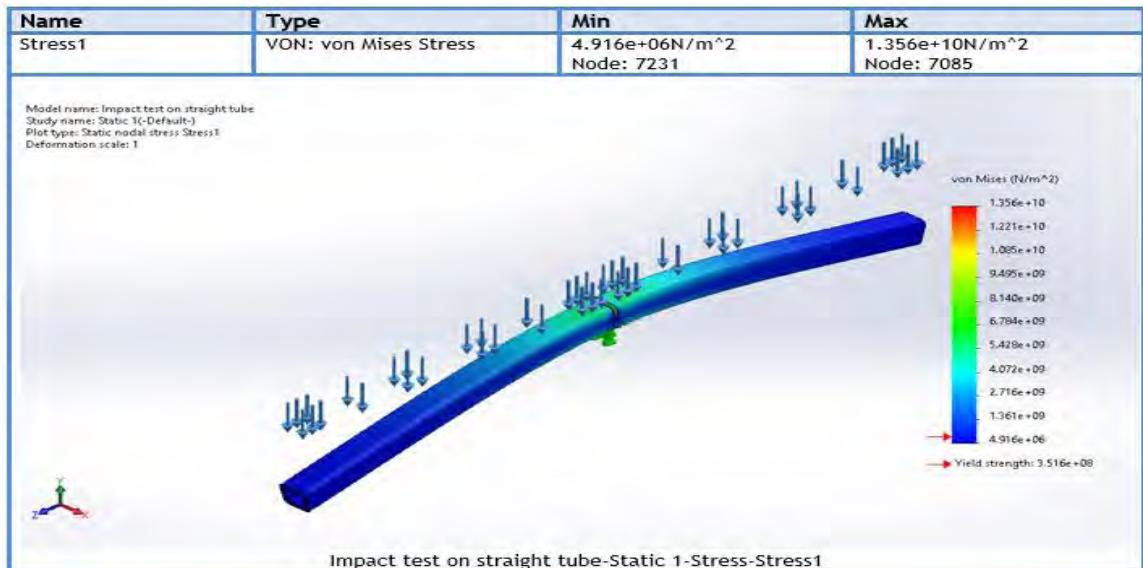
Appendix E. 18 Resultant displacement S – shape Sample

Name	Type	Min	Max
Displacement1	URES: Resultant Displacement	0.000e+00mm Node: 43	5.535e+01mm Node: 13

Impact test on straight tube-Static 1-Displacement-Displacement1

98
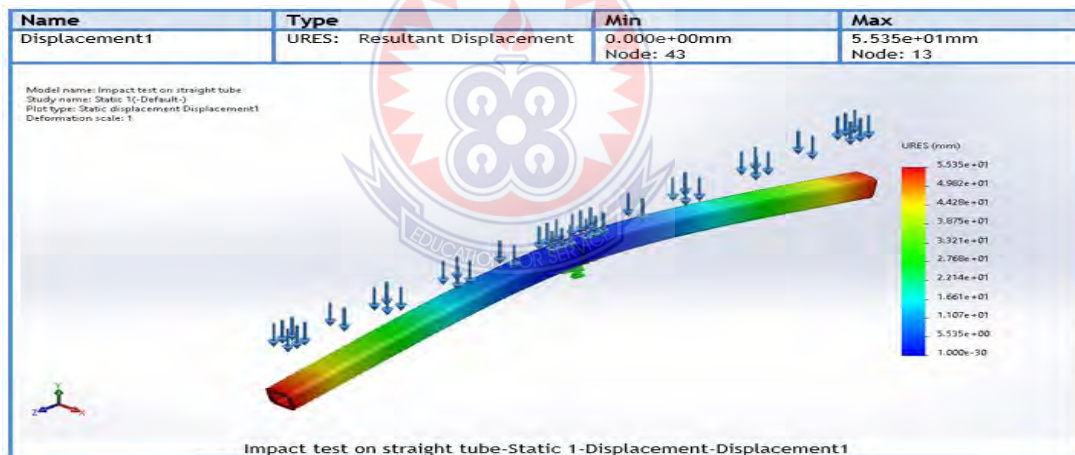
Appendix E. 19 Equivalent Strain for S – shape Sample

Name	Type	Min	Max
Strain1	ESTRN: Equivalent Strain	5.575e-06 Element: 6032	4.062e-02 Element: 1914

Impact test on straight tube-Static 1-Strain-Strain1
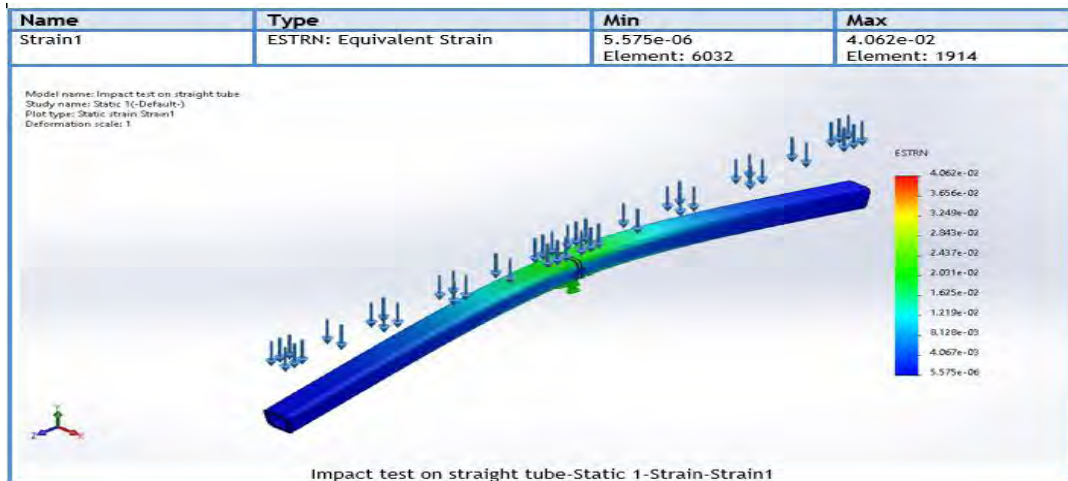
Appendix E. 20 Deformed shape for S – shape Sample

Name	Type
Displacement1{1}	Deformed shape

Impact test on straight tube-Static 1-Displacement-Displacement1{1}
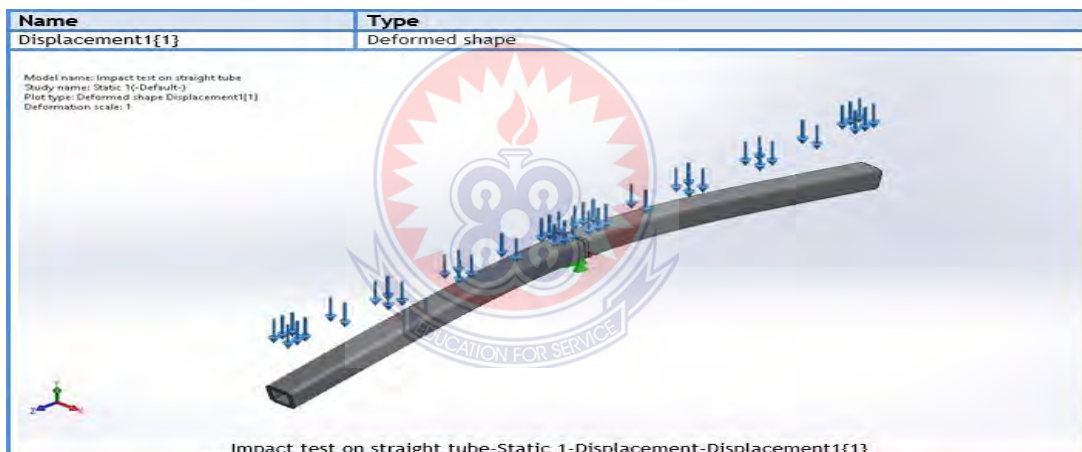
Appendix E. 21 Equation for von mises stress for S – shape Sample

Name	Type	Min	Max
Equation1	"VON: von Mises Stress"	4.916e+06SI Node: 7231	1.356e+10SI Node: 7085

Impact test on straight tube-Static 1-Equation-Equation1

99
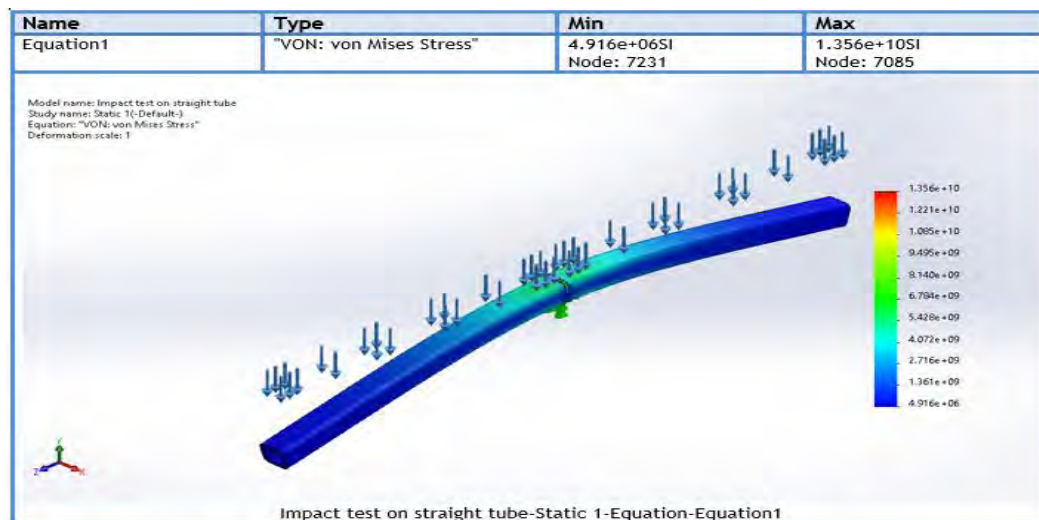
Appendix E. 22 Factor of safety for S – shape Sample

Name	Type	Min	Max
Factor of Safety1	Automatic	2.592e-02 Node: 7085	7.152e+01 Node: 7231

Model name: Impact test on straight tube
Study name: Static 1(-Default-)
Plot type: Factor of Safety Factor of Safety1
Criterion : Automatic
Factor of safety distribution: Min FOS = 0.026

FOS

7.152e+01
6.437e+01
5.722e+01
5.007e+01
4.292e+01
3.577e+01
2.862e+01
2.147e+01
1.433e+01
7.176e+00
2.592e-02

Impact test on straight tube-Static 1-Factor of Safety-Factor of Safety1

Appendix D. 23 Stress Graph for deformed C – shape Sample

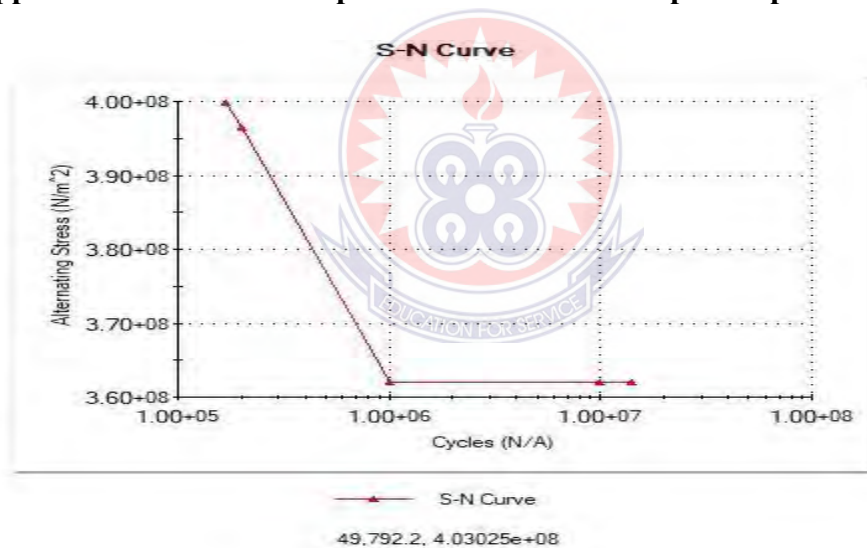S-N Curve

49.792.2, 4.03025e+08

Image-1

Figure 3.9.6 Computerized Universal Tensile Test Machine

(Source: Lab Work, November, 2020)